Chapter 1

Introduction and Review of Literature

1.1 Introduction

The hip is a ball and socket joint, in which the head of the femur rotates relative to the acetabulam in the pelvic bone. Hip replacement or arthroplasty is a surgical reconstruction procedure, in which the diseased part of the hip joint are removed and replaced by artificial component known as implant or prosthesis. In a Total Hip Arthroplasty (THA), the proximal part of the femur is replaced by a femoral component having a spherical head, whereas the socket of the pelvic bone is replaced by an acetabular component, thereby restoring the ball and socket joint. The THA has achieved an exceptional position in the field of total joint replacement that offers relief of pain and restoration of joint functions for patients suffering from osteoarthritis (arthrosis), rheumatoid arthritis, congenital deformities or post-traumatic disorders. Although this surgical procedure is recognised as one of the most successful operations over last few decades, the chances of failure are not entirely negligible. In case of a Hip Resurfacing Arthroplasty (HRA), only the articular surfaces of the femoral head and the acetabulum are replaced with prostheses. Unlike the conventional THA, more bone is preserved in the femoral head, neck and shaft. However, for both the surgical reconstruction procedure, the replacement of acetabulum is primarily a surface replacement with varying component thickness.

Over the past few decades, THA has become a standard orthopaedic surgery. The annual report of National Joint Registry for England and Wales (2012), reported a total number of 80 314 registered hip replacement in the year 2011, an increase of 5% over 2010. Out of these, 71 672 were primary hip replacement and 8 641 were revision procedure. A total number of 347 129 registered primary hip replacement, since 1979 was reported in Swedish Hip Arthroplasty Register (2011). During the past 10 year's period, from 2000 to 2010, the total numbers of hip replacements increased considerably, an estimated increase around 41% (Swedish Hip Arthroplasty Register, 2011). On an average, the increase was around 4% per year. The Australian National

Joint Replacement Registry (2012) contained information about 38 022 hip replacement in the year 2011, an increase of 5% compared to the number reported in 2010. Data extracted and analysed by American Academy of Orthopaedic Surgeons revealed a total of 514 000 hip surgery, including primary and revision, in the year 2004 only (Source: United States Department of Health and Human Services; Centres for Disease Control and Prevention; National Centre for Health Statistics). For the Indian population, the extrapolated annual incidence rate of hip replacement surgery is approximately 469 884 (Source: The American National Institute of Arthritis and Musculoskeletal and Skin Diseases). In European countries, HRA comprised between 6 and 9% of all hip replacement performed. In the year 2011, 1801 number of surface replacement was reported in the annual report of National Joint Registry for England and Wales (2012). According to the Swedish Hip Arthroplasty Register (2010), 214 cases of surface replacement of hip have been registered during 2010. A marked decrease has been noted within the period from 2007 to 2010. The Australian National Joint Replacement Registry (2012) revealed that hip resurfacing procedures accounted for 2.1% of all primary hip replacement performed in 2011. Similar to the Swedish Registry, majority of the surgery were performed on male patients (around 75%), and in patients younger than 65 years of age (around 91%).

Aseptic loosening of the acetabular component is responsible for the largest proportion of failures in THA and HRA. Some authors report the rate of acetabular component loosening to be two to three times higher than that of the femoral component (Schulte *et al.*, 1993, NJR 2010). However, in comparison to the femoral component, there has been a very few studies investigating the failure mechanisms of the acetabular prosthesis. Although clinical feedback studies indicate mechanical causes, the precise relationship between cause and the effect and the extent to which these mechanical factors play a role in the loosening process has not been well understood. Design of prosthesis involves both structural and functional considerations. The artificial joint must provide the normal range of movements while transferring the joint forces that are generally several times the body weight. The implant-bone system forms a composite structure consisting of several components and material interfaces that should last for lifetime in a patient. It is therefore, a challenging design problem that must account for the strength of the components, wear of the articulating surfaces, the strength of the material interfaces and the bone adaptation due to altered mechanical environment due to implantation. Despite the

generally inferior clinical performance of acetabular components as compared to femoral components, the failure mechanisms of acetabular reconstruction, particularly with reference to the effects of prosthesis design variables, remains scarcely investigated.

1.2 Anatomy and biomechanics of hip-joint

1.2.1 Anatomical planes and directions

The different anatomical planes and its orientations of the human body are shown in Fig. 1.1. A sagittal (median) plane is perpendicular to the ground, which separates right and left parts of the body. The transverse plane is parallel to the ground, which separates top (superior) and bottom (inferior) parts of the human body and a coronal plane or frontal plane is perpendicular to both the planes, which separates front (anterior) and back (posterior) sides of the human body. The 'lateral' and 'medial' directions are defined as the direction away and towards from the midline of the body, respectively (Fig. 1.1b). The directions towards the back and front sides of the body are termed as 'posterior' and 'anterior', respectively. The 'inferior' and 'superior' directions indicate towards the bottom and top of the body, respectively. The 'proximal aspect' is referred as the nearest to the top of the body, whereas 'distal aspect' is referred as the bottom of the body.

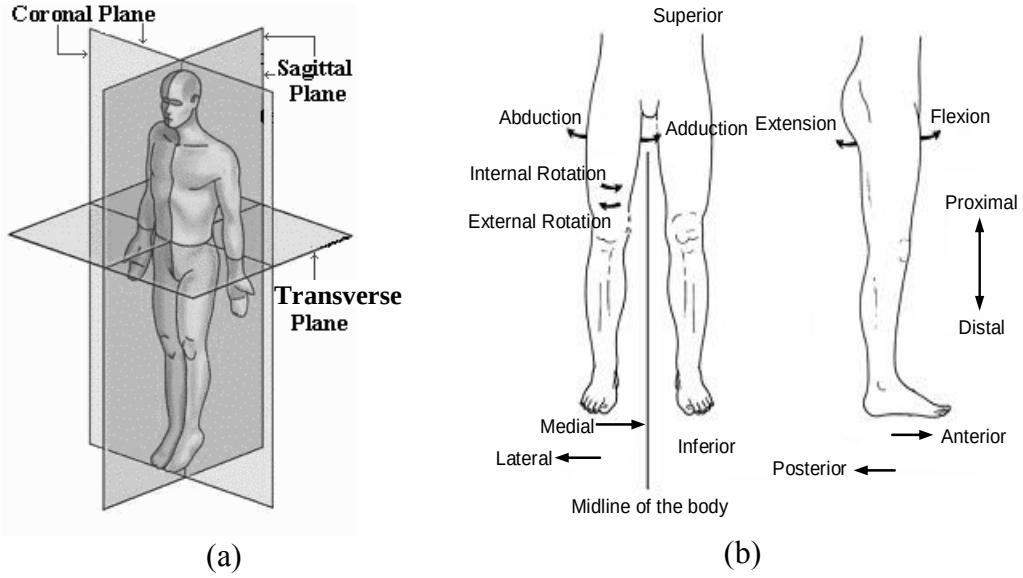

Fig. 1.1: Sketch showing (a) anatomical planes of reference; (b) anatomical directions and movements of the hip joint (Martini and Bartholomew, 2000).

1.2.2 Hip anatomy

Hip joint forms the primary connection between the bones of the lower limb and upper limb of the human skeletal system. The primary task of the hip joint is to transfer load from upper limb to lower limb. The main parts of this joint are: a ball (femoral head) which is situated at the top of the thighbone (femur) that fits into a rounded socket (acetabulum) in the pelvis (Gray, 1918). Bands of tissue called ligaments (hip capsule) connect the ball to the socket and provide stability to the joint. In the hip joint, smooth durable layers of articular cartilage cover the bone surfaces of femoral head and acetabulum, thereby providing a cushion to the ends of the bones and enabling them to move easily. Cartilage is a protein substance that serves as a "cushion" between the bones of the joints. A thin, smooth tissue called synovial membrane covers all remaining surfaces of the hip joint. In a healthy hip, this membrane makes a small amount of fluid that lubricates and almost eliminates friction in the hip joint. Normally, all these parts of the hip work in harmony, allowing painless and easy movement.

1.2.3 Structure of pelvis

The pelvic bone lies on the upper part of the hip (Gray, 1918). Therefore, it plays an important role in the load transfer across the joint. The pelvis consists of three hip bones, such as ilium, ischium and pubic bone (Fig. 1.2). One side of the pelvic bone is attached to the sacrum, connected with strong ligament. The other part is connected to another pelvis at pubis-symphasis by ligaments.

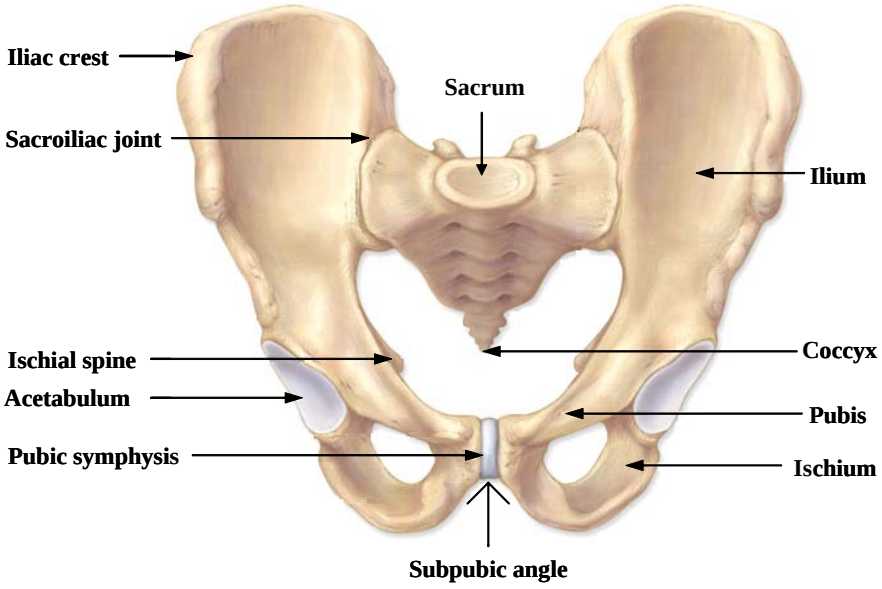

Fig. 1.2: Anatomy of pelvis; anterior view
(http://www.graphicshunt.com/health/images/)

The Ilium: The ilium is the uppermost and largest bone of the pelvis, also called iliac bone. It consists of two large broad plates, one on each side, which serves to support the internal organs, and to provide attachment of muscles back, sides and buttocks.

The ischium: The ischium forms the lower and back part of the pelvic bone. The ischium has two broad curves of bone, one on each side, which lay below the ilium, and attached to the pubis in the front and the ilium in the back. The ischium serves as a place of attachment for muscles.

The pubis: The pubic bone is located towards the frontal portion of the pelvic bone. It attaches to the ilium on the sides and the ischium on the bottom. It provides structural support and attachment site for muscles of the inner thigh. The femoral head nestles in the socket formed by these three bones.

1.2.4 Human gait cycle

The gait (human) cycle is a time interval or sequence of motion occurring from heel strike to heel strike of the same foot of a normal walking cycle. Interestingly, every individual has a unique gait pattern. The gait cycle has been broadly divided into two phases: stance phase and swing phase. These phases can then be further subdivided into eight different phases as described in terms of percentage of gait cycle. During the stance phase, which is approximately 60% of the normal walking cycle, the foot remains in contact with the ground. The cycle begins with the heel contact at the start

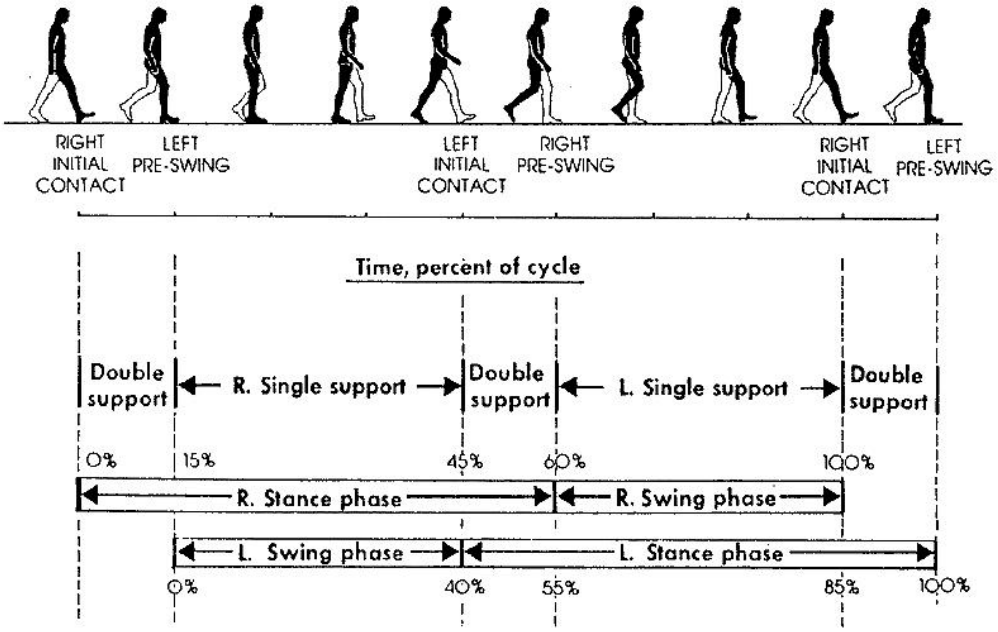

Fig. 1.3: A typical gait cycle. (Inman *et al.* 1981)

of the right foot stance phase (Fig. 1.3). The right foot is then in flat contact with the ground before the heel rises. The toe lifts off the ground after the heel and marks the end of the stance phase. Swing phase denotes remaining 40% of the gait cycle, when the foot moves in air. During the right swing phase, the left leg wholly supports the body. The swing phase ends with the heel contact and the cycle repeats itself. The same cycle applies to the left leg with a difference in time, as shown in Fig. 1.3.

In a gait cycle, the double support is the period of time when both the feet are in contact with the ground. This occurs twice in a gait cycle; once at the beginning and subsequently at the end of stance phase. The time taken for the initial and terminal double support is about 12% of the gait cycle. Single support is the time period, when only one foot is in contact with the ground. This is equal to the swing phase of the other limb, in normal walking.

1.2.5 Hip loading

Musculoskeletal loading has a predominant influence in the biological process of bone remodelling and modelling, fracture healing and primary stability of the implant (Bitsakos *et al.*, 2005; Weinans *et al.*, 2000; Duda *et al.*, 1998). A total number of twenty-one muscle forces are responsible for the movements of the hip joint. Although main purposes of these muscle forces are to producing movement during normal physiological activities and to maintain a balance of the body, some of them play a major role as far as force and torque is concerned (Nordin and Frankel, 2001). The muscles are mainly classified as flexors, extensors, abductors, adductors and dip hip external rotations according to movements they produce. Action of the dominant groups of hip muscle is presented in Table 1.1. It is important to recognize that the lines of action of each muscle between its points of origin and insertion relative to the femur will contribute to rotations additional to those indicated in the Table 1.1. Apart from these muscle forces, hip-joint force plays a predominant role in load transfer from the upper extremity to the lower extremity (Dalstra and Huiskes, 1995).

Over the past few decades, several investigators have measured the hip-joint (or hip contact) force using force plate system and kinematic data combined with electromyography (EMG) for the normal hip joint (Crowninshield *et al.*, 1978; Paul, 1967; Röhrle *et al.*, 1984; van den Bogert *et al.*, 1999) and using instrumented hip prostheses for the implanted hip joint (Bergmann *et al.*, 1993, 1995, 2001, 2004; Davy

Table1.1: Principal actions of dominant hip muscles (adapted from Dowson *et al.*, 1981).

Movement	Muscle	Origin	Insertion
Flexion	m.gracilis	Pubic bone	Anterior medial tibial condyle
	m.pectineus	Pubic bone	Pectineal line
	m.iliopsoas	Iliac fossa, anterior lumber spine	Lesser trochanter
	m.sartorius	Anterior superior iliac spine	Anterior medial tibial condyle
	m.rectus femoris	Anterior superior iliac spine	Tibial tuber via patellar tendon
Extension	m.gluteus maximus	Posterior ilium, sacrum	Iliotibial band and gluteal tuberosity
	m.biceps femoris	Ischial tuberosity, linea aspera	Fibular head
	m.semitendinosus	Ischial tuberosity	Anterior - medial tibial condyle
	m.semimembranosus	Ischial tuberosity	Medial tibial condyle
Abduction	m.tensor fascia latae	Lateral to Anterior superior iliac spine	Inserts into iliotibial band
	m.gluteus medius	Gluteal lines on posterior ilium	Greater trochanter
	m.gluteus minimus	Gluteal lines on posterior ilium	Greater trochanter
Adduction	m.adductor magnus	Inferior pubis and ischium	Adductor tuberosity, linea aspera
	m.adductor longus	Pubic bone	Linea aspera
	m.adductor brevis	Pubic bone	Upper linea aspera
Deep hip external rotators	m.piriformis m.gemellus inferior m.gemellus superior m.obturator externus m.obturator internus m.quadratus femoris	Sacrum, obturator membrane, ischium	Greater trochanter

et al., 1988; Kotzar *et al.*, 1991; Taylor *et al.*, 1997). A large amount of inter-patient variability was taken into account in most of the studies in order to measure hip contact force. The measured data of hip-joint force and torsional moments obtained by several researchers during normal life activities are summarized in Table 1.2. A significant contribution towards measurement of the hip contact force for multiple patients during normal walking and stair climbing was reported by Bergmann *et al.* (1993, 2001). Using individual patient data, an average value of the hip contact force was calculated. Measured data of Bergmann *et al.* (1990, 1993) indicated that the peak hip-joint contact force varies for patient to patient and it is ranging from 280% to 480% of the body weight (BW) during a normal walking cycle. The peak hip contact

Table 1.2: Range of peak hip contact force and torsional moments in routine activities from selected studies (adapted from Pal, 2009).

Activity	Hip contact force (% BW)	Twisting moment (% BW.m)	Instrumentation	References
Walking	260 – 280	-	Instrumented telemetric hip prosthesis	Davy *et al.* 1988
	270	-		Kotzar *et al.* 1991
	277	-		Taylor *et al.* 1997
	280 – 480[##]	1.30 – 4.40[##]		Bergmann *et al.* 1993
	211 – 285	1.20 – 190		Bergmann *et al.* 2001
	220 – 280	-	EMG/force plate	van den Bogert *et al.* 1999
	490 – 700	-		Paul, 1967
	450 – 750	-		Crowninshield *et al.* 1978
Stair climbing	260	-	Instrumented telemetric hip prosthesis	Davy *et al.* 1988
	320	-		Taylor *et al.* 1997
	350 – 550[#]	3.70 – 5.70[#]		Bergmann *et al.* 1995
	227 – 314	1.80 – 3.00		Bergmann *et al.* 2001
Jogging	550	5.30		Bergmann *et al.* 1993
Stumbling	870	5.40		Bergmann *et al.* 1993
				Bergmann *et al.* 2004
Single leg stance	210 – 280	-		Kotzar *et al.* 1991
Standing up	181 – 220	0.80 – 1.21		Bergmann *et al.* 2001
Sitting down	149 – 176	0.40 – 0.91		
Knee bend	117 – 177	0.58 – 0.83		

Notes:

[##] Upper value for walking at 5 km·h^{-1}

[#] Upper value measured in one patient only and considered abnormally high

force was found to be 238% of the BW during walking at a speed of 4 km.h^{-1} (Bergmann *et al.*, 2001). In case of stair climbing, the average measured hip contact force was slightly higher and reported to be 251% BW. The variation of the hip-joint force during a normal walking cycle is shown in Fig. 1.4. The peak hip-joint force occurred after the heel strike (approximately 13% of the gait cycle).

Apart from the hip-joint force, several researchers predicted the muscle forces during daily life activities (Brand *et al.*, 1982, 1986, 1994; Crowninshield and Brand, 1981; Duda *et al.*, 1996, 1997, 1998; Glitsch and Baumann, 1997; Heller *et al.*, 2001; Pedersen *et al.*, 1997). A mathematical optimization algorithm was used to estimate the complex distribution of *in vivo* muscle forces. A good agreement was observed between the data obtained using the optimization method and the measured EMG data of the muscles forces during normal gait (Crowninshield and Brand, 1981; Glitsch and Baumann, 1997). The hip-joint forces and twenty-one muscle forces calculated by

Table 1.3: Magnitudes (in Newton) of hip-joint force and twenty-one muscle forces for eight load cases of a gait cycle. Percentage of gait cycle corresponding to a load case is indicated within brackets.

Muscle Name	Load case 1 (2%)	Load case 2 (13%)	Load case 3 (35%)	Load case 4 (48%)	Load case 5 (52%)	Load case 6 (63%)	Load case 7 (85%)	Load case 8 (98%)
Hip-joint force	426	2158	1876	1651	1180	187	87	379
Adductor brevis	0	114	0	0	0	202	0	114
Adductor longus	0	88	0	0	88	158	70	140
Adductor magnus	0	0	0	0	132	263	0	0
Biceps femoris	298	202	88	70	123	114	79	377
Gemellus superior	140	88	123	79	0	0	158	202
Gemellus inferior	0	0	0	0	0	140	79	149
Gluteus maximus	842	930	167	377	456	491	114	482
Gluteus medius	1018	1053	1474	1509	1412	982	105	421
Gluteus minimus	228	140	263	228	175	123	114	219
Gracilis	0	0	0	0	88	158	70	140
Iliopsoas	149	0	316	403	395	447	105	140
Obturator externus	0	0	0	0	123	167	132	123
Obturator internus	167	123	0	61	61	149	123	0
Pectineus	0	0	175	96	0	149	0	0
Piriformis	202	175	0	0	0	0	123	228
Quadratus femoris	61	96	0	0	88	184	0	0
Rectus femoris	0	123	0	0	0	175	105	96
Sartorius	0	88	0	0	35	158	88	88
Semimembranosus	579	368	333	368	421	298	61	421
Semitendinosus	0	140	105	246	316	368	105	0
Tensor fasciae latae	0	132	88	158	149	88	70	96

Source: Dalstra and Huiskes, 1995.

Dalstra and Huiskes (1995), assuming 650 N as a body weight are summarized in Table 1.3. The hip-joint forces were based on the data reported by Bergmann *et al.* (1990) and the muscle forces were based on Crowninshield and Brand (1981). The directions of the muscle forces were found by Dostal and Andrews (1981).

One of the most significant contributions of hip loading came from Heller *et al.* (2001), who calculated the magnitude of muscle forces and hip contact force using optimization method for the most-frequent daily activities, such as walking and stair climbing for four patients. Although the optimization technique yielded hip contact force values (Heller *et al.* 2001), reasonably similar to measured values (Bergmann *et al.* 2001), deviations in measured and calculated values were observed throughout the entire gait cycle (Fig. 1.4b). In their study, minimizing the sum of muscle forces, as reported by Crowninshield (1978), was employed as an optimization criterion and inequality constraints were imposed on the maximum muscle forces (Challis, 1997).

In case of biomechanical analysis of long bones, the locations and the size of a muscle attachment plays an important role (Duda *et al.*, 1996). Different methods were implemented to quantify the muscles attachment size and locations (Brand *et al.*, 1982; Chao *et al.*, 1993, 1994; Crowninshiled *et al.*, 1978; Dostal and Andrews, 1981; Duda *et al.*, 1996; Lengsfeld *et al.*, 1994). Duda *et al.* (1996) determined reproducibly the muscle attachment area, centroidal location of this area and the muscle volume in six femoral specimens using a digitization method. In this computed area of muscle attachments and measured muscle volume, a wide range of inter-specimen variability was considered (Brand *et al.*, 1982; Duda *et al.*, 1996). A schematic view of the attachment sites of twenty-one muscles acting on the right hemi-pelvis is presented in Fig. 1.5. The attachment sites of twenty-one muscles are based on the data reported by Dalstra (1993), Phillips (2005) and Gosling *et al.* (2008), respectively.

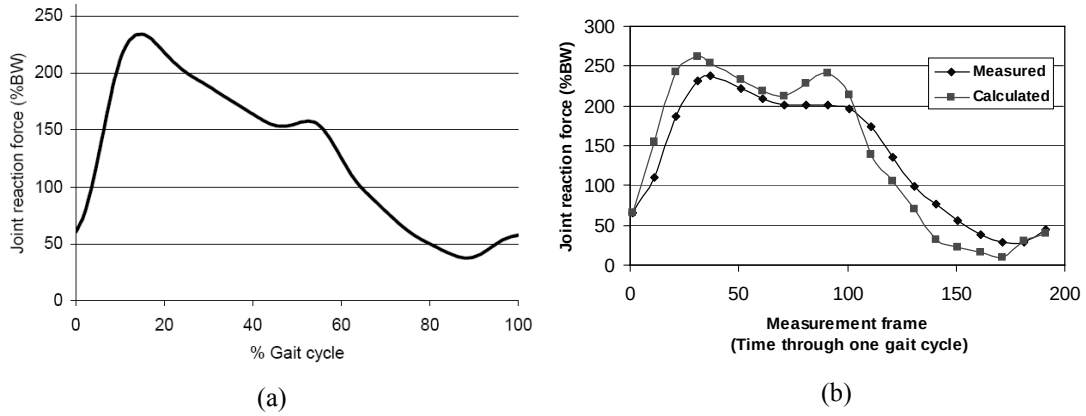

Fig. 1.4: (a) Typical joint reaction force diagram for the hip joint for normal gait; (b) comparison between calculated and measured joint reaction force (Bergmann *et al.,* 2001; Heller *et al.,* 2001).

1.3 Bone structure and properties

The primary structural element of the human body is bone. Bone has high rigidity and hardness. The main functions of bone is to support the body weight, protect internal organs, provide rigid kinematic links and facilitate attachment sites for muscles allowing movements of limbs and store essential minerals in the body. From an engineering point of view, bone is non-homogeneous, anisotropic and viscoelastic in nature. It has the ability to adapt its structure according to changes in mechanical environment, like other biological tissue. Depending on the porosity, bone exhibits wide variations in morphology.

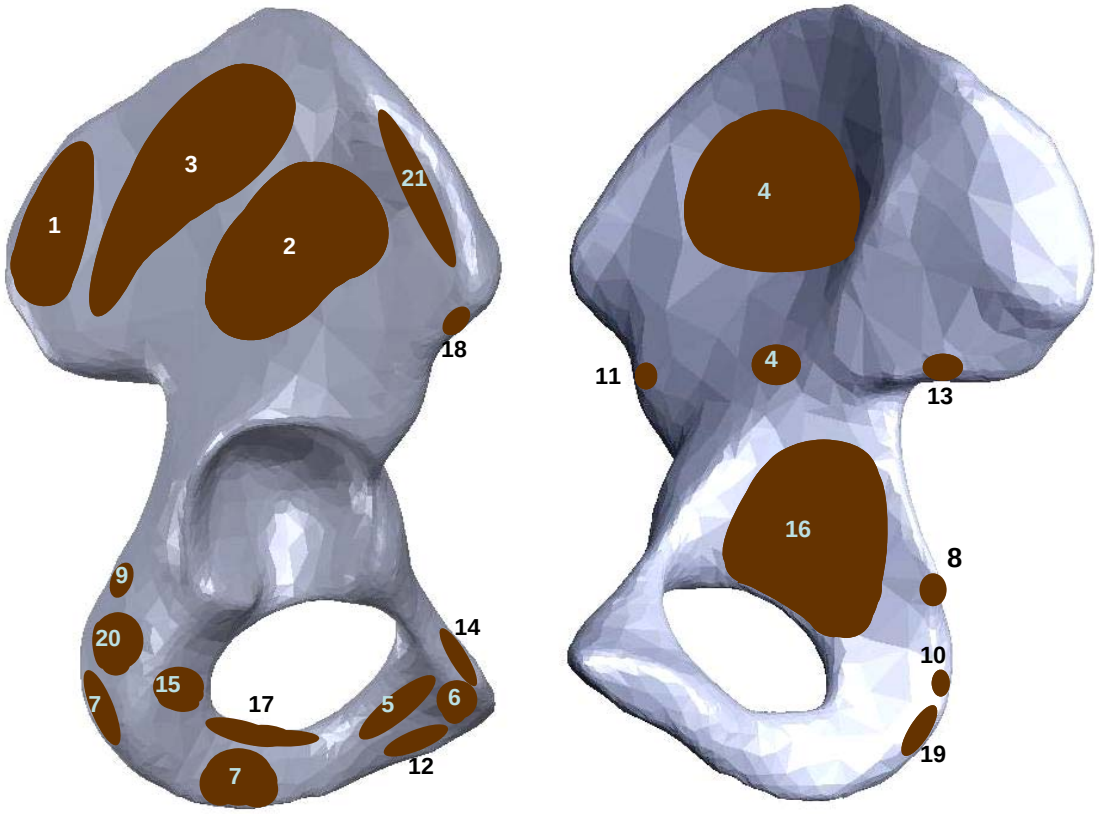

Fig. 1.5: Schematic diagram of muscle attachment sites on the pelvis; (a) lateral view; (b) medial view. (1) Gluteus maximus, (2) Gluteus minimus, (3) Gluteus medius, (4) Iliopsoas, (5) Adductor brevis, (6) Adductor longus, (7) Adductor magnus, (8) Biceps femoris, (9) Gemellus superior, (10) Gemellus inferior, (11) Rectusfemoris, (12) Gracilis, (13) Piriformis, (14) Pectineus, (15) Quadratus femoris, (16) Obturator internus, (17) Obturator externus, (18) Sartorius, (19) Semitendinosus, (20) Semimembranosus, (21) Tensor fasciae latae.

Bone is primarily composed of collagen fibres and small crystals of inorganic bone mineral calcium hydroxyapatite, $Ca_{10}(PO_4)_6(OH)_2$. Bone is a connective tissue that occurs in two forms: as a dense solid compact or cortical bone and as porous network of connecting rods and plates, cancellous bone (Gibson, 1985). This classification is based on the relative densities or volume fraction of solid. Most bones in the human body have both types, the cortical bone forming the outer shell, which surrounds a core of spongy cancellous or trabecular bone (Gibson, 1985). The volume fraction of solids greater than 70% is generally classified as compact bone, whereas the volume fraction of solids for cancellous bone is generally less than 70%. The structure of the cancellous bone is porous in nature. Depending on the anatomic locations and load carrying capability the distributions of cortical and cancellous bone varies widely from bone to bone. The compositions of mineral and organic compound have large influence on the mechanical properties of bone tissues. The stiffness of the cortical bone is dependent on the amount of hydroxyapatite (HA) present in the bone, while ductility is governed by the collagen content (Guo, 2008). Cortical bone is a solid mass of bone with microscopic channels (Gibson, 1985). In comparison, the cancellous bone has a cellular structure consisting of network of interconnecting rods and plates. This structure of rods and plates is called trabeculae, hence it is also known as trabecular bone (Gibson, 1985).

1.3.1 Mechanical properties of cortical bone

The cortical bone has a higher strength and elastic modulus in the longitudinal direction than those in the transverse directions. Ashman *et al.* (1984) measured elastic modulus of the cortical bone to be around 20 – 22 GPa along the longitudinal direction, as compared to lower elastic modulus of 12 – 14 GPa along transverse directions, indicating transversely isotropic material properties. The cortical bone is 1.5 – 2 times stiffer and stronger along the longitudinal direction as compared to radial or circumferential directions. Carter *et al.* (1981) reported that the elastic modulus of the cortical bone is in the range of 17.5 ± 1.9 GPa. Using three-point bending tests on a femur, the elastic modulus of cortical bone in the longitudinal direction was found to be in the range of 14 – 22.8 GPa (Cuppone *et al.*, 2004). Based on tensile tests carried out on femur specimens, Dong and Guo (2004) reported that the elastic modulus of cortical bone in the longitudinal and transverse directions varied in the range of 13.4 – 20.7 GPa and 6.5 – 12.8 GPa, respectively, whereas the Poisson's ratio varied in the range of 0.32 – 0.44.

1.3.2 Mechanical properties of cancellous bone

The mechanical behaviour of the cancellous bone is similar to cellular solids, such as polymeric foam (Gibson, 1985; Gibson and Ashby, 1988; Pugh *et al.*, 1973; Rajan, 1985). Bone structure consists of an interconnected network of rod and plate like trabeculae (Gibson, 1985; Gibson and Ashby, 1988). The most important feature of cancellous bone is its relative density, which is equivalent to the volume fraction of solids. At low relative densities, the structure consists of rods connecting to form open cells. At higher relative densities, the structure transforms into a more closed network of plates, where more material is accumulated in the cell wall.

The cancellous bone material properties and stress-strain characteristics are not only dependent on the apparent density; it is also influenced by the mode of loading, such as tension and compression. Three distinct regions are observed in stress-strain curve of the cancellous bone, when the mode of loading is compressive. An initial elastic region is observed first followed by a plateau region, where stress is almost constant and finally an increasingly steep region until fracture will occur (Gibson, 1985; Özkaya and Nordin, 1999). The yield point is considered as fracture of trabeculae. The study by Morgan and Keaveny (2001) and Morgan *et al.* (2003) reported that the yielding of the cancellous bone varies largely with anatomic location. Under tensile loading condition, the cancellous bone fractures abruptly, indicating brittle in nature. The cancellous bone has high energy absorption capacity under compressive loading as compared to tensile loading (Kaneko *et al.*, 2004).

Cancellous bone is a non-homogenous, anisotropic material. In order to assign material property of cancellous bone, a power law relationship between bone density and elastic modulus was examined in a series of experimental studies (Morgan *et al.*, 2003; Morgan and Keaveny, 2001, Carter *et al.*, 1977, 1987, 1989). The empirical relationships between bone density and elastic modulus used to assign bone material properties in FE models were summarised in a review by Helgason *et al.* (2008). In all of these studies, they deduced a variety of different equations by forming a simple relationship in terms of bone density and Young's modulus, $E = C\rho^D$. The constant, C varied from 1000 to 34000 and the constant D ranged between 1.14 and 3.2, depending on the anatomic sites and bones.

Table 1.4: Range of constant C and D used in the power-law regression between elastic modulus (E in MPa) and apparent density (ρ in g.cm^{-3}).

Anatomic site	Apparent density (Range)	$E = C\rho^D$	
		C (95% CI)	D (95% CI)
Vertebra (T10 – L5)	(0.11 – 0.35)	4730	1.56
Proximal Tibia	(0.09 – 0.41)	15520	1.93
Greater Trochanter	(0.14 – 0.28)	15010	2.18
Femoral Neck	(0.26 – 0.75)	6850	1.49
Pooled	(0.09 – 0.75)	8920	1.83
Pelvic trabecular bone	(0.109 – 0.959)	2017.3	2.46

Source: Morgan *et al.* (2003), Helgason *et al.* (2008).
CI denotes Confidence Interval

The bone density-elastic modulus relationships for different bones are presented in Table 1.4.

The yield strength data of the cancellous bone at different anatomic locations and loading conditions are presented in Table 1.5. It was observed that the yield strains were similar for the cancellous bone at different anatomic locations and loading conditions. A study by Turner (1989) suggested that yield strain of cancellous bone is not dependent on structural anisotropy. A further study by Turner *et al.* (1996) found that the uniform strain criteria imitate realistic density distributions in the proximal femur, which is also applicable to human bone. The experimental study by Morgan and Keaveny (2001) indicated that the strain-based criteria for the human trabecular bone may be more mathematically simple and statistically powerful. In their study, cylindrical specimens of human trabecular bone taken from different anatomic sites were tested under tensile and compressive loading and confirmed that the yield strain of cancellous bone depend on anatomic site (Table 1.5). Moreover, due to weak dependence of yield strain on the apparent density, the yield strain of cancellous bone can be considered to be uniform within a single anatomic site (Morgan and Keaveny, 2001).

Mechanical properties of pelvic trabecular bone were hardly known until the study by Dalstra *et al.* (1993). They reported that pelvic trabecular bone is not highly anisotropic, and it can be assumed as isotropic, heterogeneous elastic.

Table 1.5: Trabecular bone mechanical properties (mean ± standard deviation) by anatomic site and loading mode.

Anatomic site-Loading mode	Apparent density ($g \cdot cm^{-3}$)	Modulus (MPa)	Yield strain (%)	Yield stress (MPa)
Vertebra				
Compression	0.18 ± 0.05	344 ± 148	0.77 ± 0.06	2.02 ± 0.92
Tension	0.19 ± 0.04	349 ± 133	0.70 ± 0.05	1.72 ± 0.64
p-value	NS	NS	<0.001	NS
Proximal tibia				
Compression	0.23 ± 0.06	1091 ± 634	0.73 ± 0.06	5.83 ± 3.42
Tension	0.23 ± 0.10	1068 ± 840	0.65 ± 0.05	4.50 ± 3.14
p-value	NS	NS	<0.001	NS
Greater trochanter				
Compression	0.22 ± 0.05	622 ± 302	0.70 ± 0.05	3.21 ± 1.83
Tension	0.22 ± 0.04	597 ± 330	0.61 ± 0.05	2.44 ± 1.26
p-value	NS	NS	<0.001	NS
Femoral neck				
Compression	0.58 ± 0.11	3230 ± 936	0.85 ± 0.10	17.45 ± 6.15
Tension	0.54 ± 0.12	2700 ± 772	0.61 ± 0.03	10.93 ± 3.08
p-value	NS	NS	<0.001	0.003

Source: Morgan and Keaveny (2001).
NS indicate no significant differences ($p>0.05$)

The following density elastic modulus relationship was used to accurately define the mechanical properties of pelvic trabecular bone.

$$E = 2017.3\ \rho^{2.46} \quad \ldots. (1.1)$$

Later, this relationship was successfully used by several researchers in the 3-D FE models in order to assign material properties of the pelvic cancellous bone (Anderson *et al.*, 2005; Leung *et al.*, 2009; Zhang *et al.*, 2010). More recently, Zhang *et al.* (2010) developed and validated a 3-D FE model of a pelvis using both homogeneous and heterogeneous material property distributions for the cancellous bone. The model, having heterogeneous material property (using equation 1.1), predicted a closer agreement with the measured strain values as compared to those predicted by the homogenous bone model.

1.4 Review of literature: hip arthroplasty

In 1925, a surgeon in Boston, M.N. Smith-Petersen, moulded a piece of glass into the shape of a hollow hemisphere which could fit over the ball of the hip joint and provide a new smooth surface for movement. A remarkable improvement was made in 1936 when scientists manufactured a cobalt-chromium alloy which was almost immediately applied to orthopaedics. While this new metal proved to be a great success, the actual resurfacing technique was found to be less than adequate. The search for different types of prostheses continued. The modern artificial joint owes much to the work of Sir John Charnley, an innovative surgeon from England. His work in the field of tribology resulted in a design that completely replaced the other designs by the 1960s. Charnley's design consisted of three parts – (1) stainless steel femoral component (2) an Ultra High Molecular Weight Polyethylene (UHMWPE) acetabular component (initially PTFC and HDPE), both of which were fixed to the bone using (3) bone cement. That was the true birth of THA. The small femoral head of 22.25mm diameter was chosen for its reduced wear rate. However, this suffered from poor stability.

1.4.1 Acetabular replacement: state-of-the-art

During the period 1970s to 1980s, the second generation acetabular implant was introduced by Amstutz, Furuya and Freeman (Amstutz *et al.*, 1977, 1978, 1989; Freeman *et al.*, 1978; Furuya *et al.*, 1978). Polyethylene (HDPE/UHMWPE)-on-metal bearing surface was used and cemented fixation was employed for both the components. Although the femoral component was performing well, problems were observed in the acetabular side. In comparison to the femoral components, the rate of aseptic loosening for the acetabular components increased with time (Engh *et al.*, 1990; Mulroy and Harris, 1990). The high rate of acetabular cup loosening was primarily caused due to wear debris induced periprosthetic osteolysis (Amstutz *et al.*, 1994; Mai *et al.*, 1996).

In 1991, Heinz Wagner introduced the cementless implant, consisted of high carbon containing wrought-forged Co-Cr alloy articulating surface with a titanium alloy metal backing (Wagner and Wagner, 1996). In the same year, McMinn *et al.* (1996) introduced cementless MoM hip resurfacing implant. In the year 1992, the components were modified with HA coating. Later, McMinn introduced an all cemented system modifying the macrofeatures of the original acetabular component.

However, this cemented design had a high incidence of acetabular loosening due to cement-cup debonding, which led to the development of hybrid system of HRA, with cementless HA coated acetabular cup. In 1996, Harlan Amstutz introduced another hybrid hip resurfacing (Conserve Plus; Wright Medical Technology, Arlington, Tennessee, USA). Cast heat treated and solution annealed Co-Cr alloy was used for both the components and the acetabular cup had sintered Co-Cr beads on its outer surface (Amstutz *et al.* 2004). The modern-day commercial acetabular component designs, such as PINACLE and DURALOC (Depuy International, Leeds, UK), DUROM (Zimmer, Warsaw, IN, USA), ADEPT hip system (Finsbury Orthopaedics, Surrey, UK) are also based on MoM articulation. However, the essential differences between the designs were related to metallurgical composition, bearing geometry and fixation method of the components.

It is well understood that hard-on-hard material combinations, such as metal-on-metal, metal-on-ceramic and ceramic-on-ceramic generate less volumes of wear than hard-on-soft bearing, such as metal-on-polyethylene. However, question was raised regarding the long-term clinical effect of metal ions released from MoM bearings, which may react with body fluid. Moreover, excessively stiff implants (metal or ceramic) generally alter the strain field in the peri-prosthetic bone, leading to bone resorption and subsequent implant loosening (Huiskes *et al.*, 1992). In order to overcome these problems, composite materials evolved as the alternative to metallic, ceramic or polyethylene (PE) acetabular components, since its elastic modulus (E) is more close to that of the host cortical bone ($E \approx 17GPa$) and it offers the potential to fabricate components with specific requirements (Field and Rushton, 2005; Field *et al.*, 2006, 2008; Manley *et al.*, 2006; Manley and Sutton 2008; Latif *et al.*, 2008). Development of highly cross-linked UHMWPE has shown improved performance (Kurtz, 2009; Min *et al.*, 2013; Babovic and Trousdale, 2013).

During the last decade, flexible, wear resistant, anatomic shaped acetabular components fabricated from polymer composites have evolved. The composite cups would allow for more deformation and less peri-prosthetic bone loss than metal backed PE, metallic and ceramic hemispherical components (Morscher *et al.*, 1997; Brooks *et al.*, 2004; Field and Rushton 2005; Field *et al*., 2006, 2008; Manley *et al.*, 2006; Manley and Sutton 2008; Latif *et al.*, 2008; Dickinson *et al.*, 2012). The intact acetabulum is subjected to large amount of elastic deformation due to the action of

musculoskeletal loads during physiological activities (Konrath *et al.*, 1998). Considering these requirements, the horseshoe-shaped Cambridge cup, made of carbon-fibre reinforced Polybutyleneterephthalate (CFR-PBT) with UHMWPE articulating surface, was designed to replace the articular cartilage of the acetabulum and the underlying subchondral bone. The Cambridge cup design was modified later, in which UHMWPE layer was removed from the articulating surface to avoid interface debonding between two materials and high volumetric wear rate of UHMWPE (Latif *et al.*, 2008). The modified acetabular component, known as MITCH PCR^{TM} cup, consisted of two parallel fins and made of only carbon-fibre reinforced polyetheretherketone (CFR-PEEK) material, was reported to have better wear resistant properties (Scholes and Unsworth 2007; Scholes *et al.*, 2008). However, more rigorous investigations are required to evaluate the performance of these types of acetabular prostheses.

1.4.1.1 Reasons for hip replacement

The main reason for hip replacement surgery is joint pain, caused due to a diseased hip joint. As a consequence, a patient has limited ability to perform normal activities. Hip arthroplasty eliminates pain and improves mobility of patients suffering from common hip diseases, as described in the following:

Osteoarthritis (OA) is the most common reason for hip replacement. This bone degenerative disease, also known as degenerative arthritis or osteoarthrosis, causes mechanical abnormalities involving degradation of joints, including articular cartilage and subchondral bone. The main symptoms of OA include joint pain, tenderness, stiffness, locking, and sometimes an effusion. The causes of OA are hereditary, developmental, metabolic, and mechanical, which may initiate processes leading to loss of cartilage. As a result of decreased movement secondary to pain, regional muscles may atrophy, and ligaments may become more lax. Treatment generally involves a combination of exercise, lifestyle modification, and analgesics. If pain becomes debilitating, joint replacement surgery may be used to improve the quality of life.

Rheumatoid arthritis (RA) is a long-term disease, which causes inflammation of the joints and surrounding tissues or organs. The most affected regions are the flexible (synovial) joints, both weight bearing and non-weight bearing, leading to damage of the joint, pain and swelling. RA affects the synovial membrane, which becomes

inflamed releasing enzymes that digest bone and cartilage, leading to damage of the joint surface and eventual deformation of the joint. This disease is more common in female as compared to male, having age between 30 to 60 years.

Osteonecrosis (ON) (also called as aseptic or avascular necrosis) is a disease caused by insufficient blood flow to bones in the joints and as a result, the bone cells may die due to the lack of oxygen and nutrients. The main reason behind this disease is unknown. The main risk factor of this disease includes, long-term steroid treatment, patients who had a fracture or a dislocation around the hip or with a history of heavy use of alcohol. In early stages, it will be difficult to find ON using x-ray. In advanced stages, it shows joint destruction as similar to OA. Initial treatments of this disease include the use of walking aids, in order to reduce the load on the synovial joint. No herbal treatments for ON have been established yet. Only surgical procedure is the major course for the treatment of ON, which include joint replacement, osteotomy of the bone and bone grafts. There are other reasons for hip surgeries including femoral neck fracture due to trauma.

1.4.2 Failure scenarios

Aseptic loosening of the acetabular component is responsible for the largest proportion of failures of Total Hip Replacement (THR). The initiation of the failure process may be due to mechanical causes. Three dominant failure scenarios, as suggested by Huiskes (1993), are presented in the following.

Accumulated damage failure scenario: The likelihood of mechanical failure depends on the stresses induced within an implant material or at various material interfaces within the implant-bone structure, as compared to the strength of the material or the respective material interface. These implant materials or interfaces are too weak to sustain the effect of long-term, dynamic loads due to normal physiological activities. As a result, mechanical damage, typically micro-cracks, is gradually accumulated within the implanted bone structure, eventually causing failure. These micro-cracks reduce the strength of the cement and its bonds at the layer of interface between implant and bone, eventually causing failure. In case of uncemented prostheses, loosening may occur due to the failure of the implant-bone interface as well as the PE-metal interface. The PE cup may be dissociated from the metal-backing, which may still maintain a secure fixation with bone, thus resulting in failure of the prosthesis. The eventual gross loosening of the implant may be due to the cement-

bone interface loosening, failure (cracking) of the cement due to excessive stresses, and relative motions between the materials.

Particulate-reaction failure scenario: There are three possible sources of generation of wear particle debris in joint replacement, (1) wear of articulating surfaces, (2) abrasion of cement/prosthesis/bone interfaces, and (2) fretting between metal parts in modular prostheses. As a result of the generation and migration of these wear particle debris, the cement-bone interface gradually disintegrates, causing interfacial micro-motion and eventual mechanical loosening.

Stress/Strain shielding and bone remodelling: The implant takes the bulk of the load formerly transferred to the bone, thereby shielding the bone from the load. This evokes abrupt changes in the mechanical environment within bone, eventually causing bone resorption and osteolysis. This phenomenon, related to long-term failure of the implant, is known as adaptive bone remodelling.

1.4.3 Adaptive bone remodelling

Bone has the capability to adapt its structure (external geometry and internal structure) in response to change in mechanical loading by bone apposition (formation) and bone resorption (loss). Bone apposition and resorption occur through cellular activities of osteoblasts and osteoclasts, respectively. This adaptive process of change in bone structure is generally known as adaptive bone remodelling. The process is usually described as occurring relative to the internal morphology (internal remodelling) or the periosteal geometry (external remodelling) (Weinans, 1991). Internal remodelling is expressed as change in bone density (Carter *et al.* 1989; Huiskes *et al.* 1987), whereas external remodelling refers to changes of shape or external geometry of bone (Hart *et al.* 1984; Hart and Davy, 1989). Although these two processes occur simultaneously, for an adult person, the changes in geometry is minimal as compared to internal remodelling. The cancellous bone usually has a higher rate of metabolic activity and appears to respond more rapidly to changes in mechanical loads than the cortical bone (García *et al.,* 2002). For this reason, studies on bone remodelling have been mainly focussed on the internal remodelling process, although a few studies have investigated the combined effect of internal and external remodelling models, simultaneously (Beaupré *et al.,* 1990a; Fridez *et al.,* 1998; García *et al.,* 2002; Huiskes *et al.,* 1987; Weinans *et al.,* 1993). In case of natural bone, the rates of bone adaptation and bone resorption remain in equilibrium;

therefore, no net changes in bone morphology may occur (Frost, 1964; Parfitt, 1984; Weinans, 1991). Any change in the mechanical loading environment of bone due to insertion of a prosthesis disturbs the normal state of equilibrium prevailing in a natural bone. Implantation leads to major alterations in the stresses and strain within the reconstructed bone. Post-operatively, the prosthesis carries a part of the load which was earlier carried exclusively by the natural bone. Thereafter, bone strives to reach a new actual state of equilibrium by adapting its structure.

External loading conditions have a predominant effect in the regulation of bone remodelling process (Duncan and Turner, 1995; Huiskes *et al.,* 1989; Mullender *et al.,* 2004; Nomura and Takano-Yamamoto, 2000; Turner and Pavalko, 1998). A relationship between mechanical forces (body weight) and bone morphology was observed by Galileo in 17^{th} century (as cited by Carter, 1984; Treharne, 1981). Considerable scientific interest was developed over the last centuries, in order to describe the relationship between the structure and function of bone. Subsequently, a significant contribution evolved from Wolff (1892), blended with the theory of functional adaptation developed by Roux (Roesler, 1981; Roux, 1881). These studies concluded that bone apposition and resorption is a biologically controlled process, which is dependent on the local state of stress (Roux, 1881). Wolff hypothesised that every change in the form and the function of a bone is followed by certain definite changes in their internal architecture and equally definite secondary alterations in their external geometry, in accordance with mathematical laws (Wolff, 1892). This proposed 'law of bone transformation' by Wolff was later referred to as the 'Wolff's Law'. Over the last few decades, several researchers tried to mathematically formulate this law in order to quantify the bone remodelling process (Beaupré *et al.,* 1990a; Cowin and Hegedus, 1976; Doblaré and García, 2002; Fyhrie and Carter, 1986; Hart *et al.,* 1984; Hart and Davy, 1989; García *et al.,* 2001; Huiskes *et al.,* 1987; Jacobs *et al.,* 1997).

The theory of bone remodelling assumes that bone possess sensing capability to measure the internal change in mechanical environment (stimulus). It can respond to the change (combined with other biological factors) by the actions of osteoblasts and osteoclasts. Most studies used bone apparent density (ρ) as the variable to represent the remodelling state. However, the definition of mechanical stimulus varied for different models. Mechanical stimuli have been defined as a function of strain, stress,

strain energy density (SED), elastic strain energy per unit bone mass to predict bone adaptations (Carter *et al.,* 1989; Cowin and Hegedus, 1976; Fyhrie and Carter, 1986; Huiskes *et al.,* 1987; Weinans *et al.,* 1993). In the theory proposed by Cowin and Hegedus (1976), the objective was described as a normalisation of the active local strain values (remodelling stimulus) to the strain values corresponding to normal physiological conditions at the same locations. This approach of the remodelling objective is known as 'site-specific', since the normalised strains are site dependent. Later a similar theory was proposed by Huiskes *et al.* (1987), where the local SED was considered as the remodelling signal, instead of strain tensor, to predict bone adaptation around implants.

Another theory was introduced by Fyhrie and Carter (1986) assuming that the tissue strives to optimize its state of stresses and strain to a uniform stimulus level calculated over its entire volume. This 'non-site specific' approach was used to describe the remodelling process for any configuration without referring to the 'normal' condition. This formulation implies that bone morphology, in normal and implanted conditions, is solely dependent on the external loading conditions. However, the variable 'elastic strain energy per unit of bone', which is SED normalised to bone apparent density, was suggested as the mechanical stimulus.

The study by Frost *et al.* (1964) reported that the bone does not react to small deviations in the mechanical stimulus. A minimal threshold value of the inhibitory signal, the difference in mechanical stimuli for altered and natural conditions, is required for the initiation of bone remodelling process (Huiskes *et al.,* 1987). Bone does not react in this range of values, which is called the 'dead zone' or 'lazy zone'. This study by Huiskes *et al.* (1987) accounted for the 'dead zone', by assuming that a certain threshold level of deviation from the natural stimulus must be overcomed by the SED before net remodelling can start. The theory of bone remodelling was incorporated in iterative computer-simulation schemes, in combination with the FE analysis to predict adaptive bone remodelling around hip prostheses (Huiskes *et al.,* 1987; van Rietbergen *et al.,* 1993). However, bone was assumed to be an isotropic material in these theories.

The trabecular orientation is influenced by heterogeneous bone density distributions, leading to anisotropic continuum material properties (García *et al.* 2002). Beaupré *et al.* (1990a, b) defined a daily tissue level stress stimulus as the

equilibrium state for a time dependent remodelling theory, considering anisotropic strain data reported by Carter (1978). An anisotropic model was developed by Jacobs *et al.* (1995a, 1997) based on density adaptation and anisotropy reorientation using the principal stresses as the mechanical stimulus. Damage-based theoretical models have also proved to be capable of successfully predicting some aspects of bone remodelling (Prendergast and Taylor, 1994; Prendergast and Huiskes, 1995). Based on damage repair theory, Doblaré and García (2002) investigated an anisotropic bone remodelling theory, where microdamage in the bone surface was accounted for the remodelling stimulus. A recent study by McNamara and Prendergast, (2007) included both strain and microdamage to be explored as remodelling stimulus. Structural topology optimization is also being investigated for bone remodelling simulation (Bagge, 2000; Fernandes *et al.,* 1999; Hollister *et al.,* 1994; Jang and Kim, 2008; Jang *et al.,* 2009).

1.4.3.1 Mathematical formulation of the bone remodelling process

In all the proposed mathematical formulations, the changes in apparent density (ρ) were considered to represent the remodelling state. The mathematical formulation of bone remodelling process is based on Wolff's Law (Wolff, 1892). The theory of adaptive bone remodelling assumed the elastic strain energy per unit of bone mass as

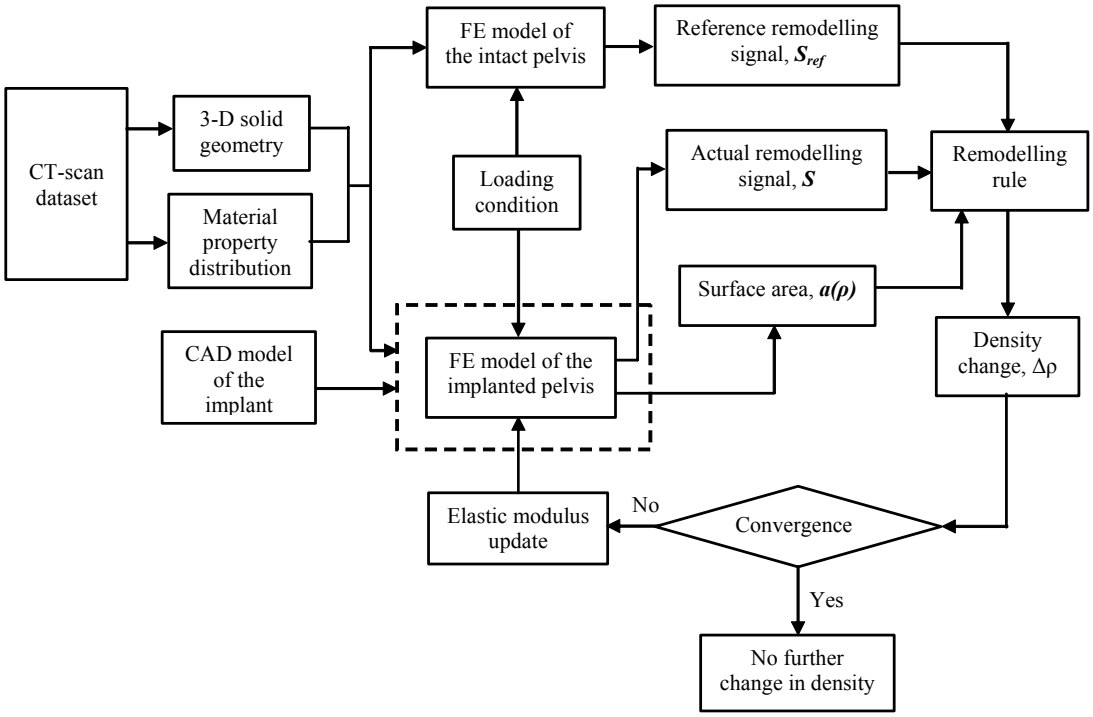

Fig. 1.6: Scheme of iterative bone remodelling simulation programme.

the mechanical stimulus (Cowin and Hegedus, 1976; Carter *et al.*, 1989; Huiskes *et al.*, 1987). A mathematical description of the bone remodelling process, in combination with an FE analysis, is schematically presented in Fig. 1.6 (Suarez *et al.*, 2012; Huiskes and van Rietbergen, 1995).

The reference stimulus S_{ref} of each bone element is obtained from the intact bone model, which is compared with the remodelling stimulus S of the corresponding bone element for the implanted bone model. The amount of bone remodelling is dependent on the difference between S and S_{ref}, and the dead zone s. After each iteration, a new model is obtained having updated bone material properties. From this updated model, a new S is determined. This iterative procedure is continued until a new equilibrium state is reached, where no more density changes would occur. The elements having mechanical stimulus within the dead zone and limiting density values of 0.01 g.cm^{-3} (no-bone condition) and 1.73 g.cm^{-3} (cortical bone), do not take part in this process.

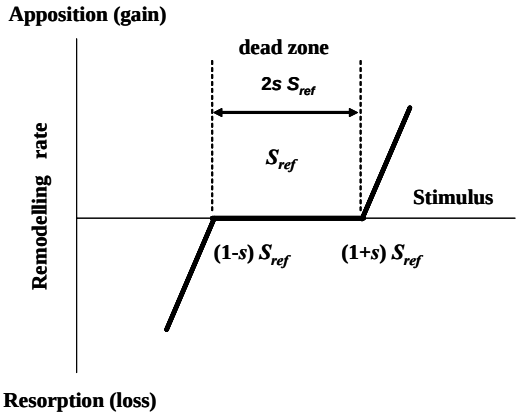

Fig. 1.7: The relationship between stimulus and rates bone resorption and apposition used in the bone remodelling simulation.

The reference stimulus (S_{ref}) and the remodelling stimulus (S) are the local (per element) elastic strain energy (U) per unit of bone mass averaged over a loading history (n), for an intact and implanted pelvis, respectively. The mechanical stimulus for each element is calculated from the FE model outputs. Owing to variations of the hip and muscle loads, the strain energy density, U, varies in each location over time during a gait cycle, due to variations in the hip-joint force and muscle loads. In order to take some of these variations into account, an average strain energy density, U_a, for a number of loading cases was used to calculate the remodelling stimuli (Carter *et al.,* 1989; van Rietbergen *et al.,* 1993), by

$$S = \frac{1}{n}\sum_{1}^{n}\frac{U_i}{\rho} = \frac{U_a}{\rho} \qquad \ldots(1.2)$$

Bone is unresponsive in some region, which is known as 'lazy zone' or 'dead zone' (Beaupré *et al.,* 1990a; Cowin, 1987; Huiskes *et al.,* 1987; van Rietbergen *et al.,* 1993) and denoted as *s* (Fig. 1.7). The idea is that bone needs a minimal threshold of the inhibitory signal, represented by S - S_{ref}. In order to determine the pore surfaces from the apparent density, Martin (1972) presented a method to calculate the internal surface area as a function of apparent density ($A = A(\rho)$). In addition, he assumed that the rate of internal geometry adaptation is dependent on the amount of internal free surface area available. The rate of mass change at the internal bone pore surfaces is linearly dependent on the amount of free surface area. The internal free surface area per unit volume of the whole bone, $a(\rho) = A(\rho)/V$, was estimated using Martin's assumptions. It is assumed that $a(\rho) = 0.0$ for $\rho = \rho_{\max} = 1.73\,\text{gm/cm}^3$, hence no remodelling takes place. Thus remodelling does not take place inside the cortical bone with an apparent density of 1.73 gm/cm^3. The relationship between the free surface area per unit volume with apparent density is presented in Fig. 1.8.

The adaptive process in the operated bone is expressed as the rate of change of bone mass.

$$\frac{dM}{dt} = \tau\, A(\rho)\left[S - (1-s)S_{ref}\right], \qquad \text{if} \quad S \le (1-s)S_{ref} \qquad \ldots (1.3a)$$

$$\frac{dM}{dt} = 0 \qquad \text{if} \quad (1-s)S_{ref} < s < (1+s)S_{ref} \qquad \ldots (1.3b)$$

$$\frac{dM}{dt} = \tau\, A(\rho)\left[S - (1+s)S_{ref}\right], \qquad \text{if } S \ge (1+s)S_{ref} \qquad \ldots (1.3c)$$

$$0.01 \le \rho \le 1.73\,\text{gm/cm}^3$$

The parameter τ is a time constant given in gm/(mm^2(J/gm)month), $A(\rho)$ is the free surface at the internal bone structure (Martin, 1972, 1984). The time *t* is given in units of one month.

Now, the rate of change of bone mass $\frac{dM}{dt}$ is expressed as a rate of change in the internal bone mass due to porosity change,

$$\frac{dM}{dt} = V\frac{d\rho}{dt} \qquad \ldots (1.4)$$

with V as the volume in which the bone mass change take place (the volume of the element) and $\frac{d\rho}{dt}$ the rate of change in apparent density.

The mathematical expression for apparent density change is described as follows:

$$\Delta\rho = \begin{cases} a(\rho)\{S-(1\pm s)S_{ref}\}\tau\Delta t, & if \quad S\leq(1-s)S_{ref} \quad or \quad S\geq(1+s)S_{ref} \\ 0, & if \quad S_{ref}(1-s)<S<S_{ref}(1+s) \end{cases} \quad \ldots (1.5)$$

The above equation (1.5) can be solved iteratively using Euler's forward integration to yield a new value of apparent density for a bone element after an iterative step. Thus, a chosen time step Δt and apparent density in each element can be determined using the following equations:

$$\Delta\rho_i = \tau\, a(\rho)\{S-(1\pm s)S_{ref}\} \qquad if \quad S\leq(1-s)S_{ref} \text{ or } S\geq(1+s)S_{ref} \quad \ldots (1.6a)$$

$$\rho_{i+1} = \rho_i + \Delta\rho_i \qquad if \quad S\leq(1-s)S_{ref} \text{ or } S\geq(1+s)S_{ref} \quad \ldots (1.6b)$$

The integration was carried out in steps of 'simulation time scale' $\tau\Delta t$ (Weinans *et al.*, 1993; Suarez *et al.*, 2012). The time step (Δt) was variable and was determined in each iteration using the following equation, where the maximum bone density change in the most highly stimulated element was assumed to be equal to the half of maximum bone density ($\frac{1}{2}\rho_{\max} = 0.865\ g.cm^{-3}$) (Weinans *et al.*, 1993).

$$\tau\Delta t = \frac{0.865}{\{a(\rho)(S-(1\pm s)S_{ref}\}_{\max}} \quad \ldots (1.7)$$

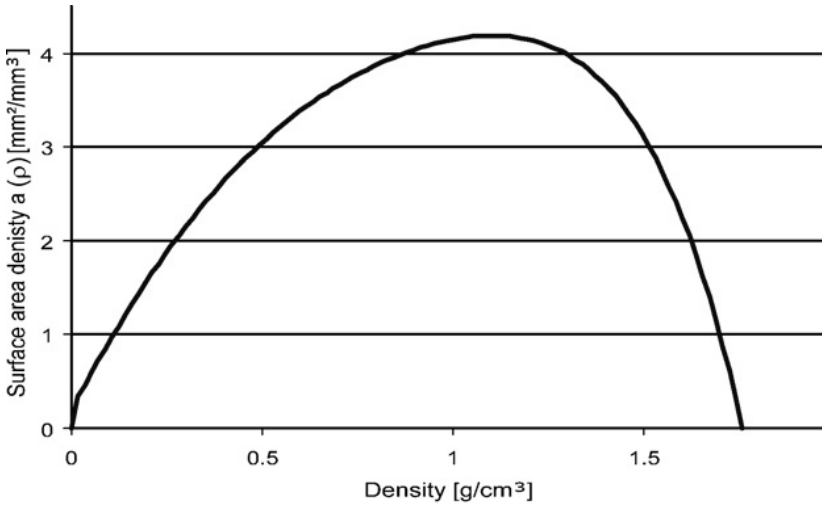

Fig.1.8: Martin's equation relating free surface area per unit volume with apparent density (Scannell and Prendergast, 2009).

The adaptation rate (τ) was assumed to be equal to 129.6 g.mm^{-2} (J/g) months for calculating Δt (Weinans et al., 1993). Thereafter, these parameters are utilized in eq. (1.5) to calculate a new apparent density value for a bone element, after each time step. Bone is modelled as continuous material at all times, the porous structure of bone is accounted by the apparent density variable and it is related to the Young's modulus (E) according to $E = C\rho^D$ (Table 1.4), where C and D are constants; E is expressed in MPa and the ρ in g.cm^{-3}.

1.4.4 Clinical studies on acetabular component

Both cemented and cementless acetabular components are used in THA and HRA. Although cemented cups are largely preferred for elderly patients with poor bone quality, cementless fixation has evoked considerable clinical interest for younger patients (Engh *et al.*, 1990; Mulroy and Harris, 1990). Aseptic loosening remains the primary cause of failure in hip arthroplasty. For cemented components, although improved cementing techniques led to marked reduction in loosening rates of 3% for the femoral components, the incidence of acetabular loosening of 42% were high and remained unchanged (Mulroy and Harris, 1990). In contrast, a four to seven years clinical follow-up study by Dorr *et al.* (2000) reported no acetabular component failure with the use of Metasul metal-on-metal articulation and a cemented Weber cup. A recent clinical study by Angadi *et al.* (2012) indicated that the patients with cemented all-PE cups and cementless porous-coated PE lined acetabular components have similar long-term clinical outcomes. The study reported 86.8% survivorship in 183 cases, implanted with cemented PE cups, in patients with a mean age of 71.3 years, ten years post-operatively. A similar result of 89.2% survivorship was observed in 104 patients with an average age of 69.8 years for the same follow-up period, implanted with Co-Cr porous coated cups.

The use of cement (PMMA) for the fixation of the implants has some disadvantages, such as bone thermal injury, necrosis and low tensile strength of the cement-bone interface. Cement is weak in tension, but strong in compression. It is the most likely material where crack is initiated. Moreover, the implant-cement interface has often been reported as the weakest link in the implanted bone, leading to interface debonding. Cement particles abraded from the cement mantle cause particulate reactions by macrophages, osteolysis, soft-tissue interposition and eventual loosening. In order to overcome these problems, cementless implant with porous or HA coated

Table 1.6: Clinical studies of uncemented acetabular component (upgraded from Lian *et al.*, 2008).

Authors	Year	Number of hips	Follow-up	Remarks
Silverton *et al.* (1996)	1996	138	8.3	0.7% loosening
Garcia-Climbrelo (1999)	1999	65	8.3	10.8% failure; 27.7% radiographic loosening
Leopold *et al.* (1999)	1999	138	10.5	1.8% radiographic loosening
Whaley *et al.* (2001)	2001	89	7.2	4.5% loosening
Templetion *et al.* (2001)	2001	61	12.9	3.5% radiographic loosening
Elke *et al.* (2003)	2003	123	7.4	4.8% failure
Della Valle *et al.* (2004)	2004	138	15	13.8% failure
Hallstrom *et al.* (2004)	2004	122	12.9	4% radiographic loosening
Morag *et al.* (2005)	2005	63	9.9	5.9% failure (normal centre); 17.7% failure (high centre)
Dorairajan *et al.* (2005)	2005	50	2.7	6% failure (recurrent dislocation)
Kim *et al.* (2008)	2008	200	19.5	5% loosening
Browne *et al.* (2010)	2010	37	3	22% failure due to aseptic loosening
Long *et al.* (2010)	2010	206	2	14.5% loosening
Bliss *et al.* (2011)	2011	98	15	31% failure

components have evolved. A summary of some clinical studies with uncemented acetabular component and its failure rate are presented in Table 1.6. It has been observed that the loosening rate of femoral components decreased with time, whereas acetabular loosening tended to increase (Engh *et al.*, 1990). Overall, acetabular component loosening has been indicated as the main cause of failure in hip replacements (Kim *et al.*, 2008; Browne *et al.*, 2010; Long *et al.*, 2010).

A study of 200 hips by Kim *et al.* (2008) reported that 14 (7%) revision required at a mean time of 19.5 months (range, 3 – 47 months) with use of metal-on-metal hip resurfacing component (CONSERVE®PLUS, Wright Medical Technology, Arlington, Tenn). Out of 14 patients, 10 failures were related to early acetabular loosening. Browne *et al.* (2010) reported 22% failure out of 37 patients due to aseptic loosening of the acetabular component at a mean follow-up of 3 years using MoM hip resurfacing component. The study by Long *et al.* (2010) using MoM articulation (DUROM®), reported 30 acetabular component loosening out of 206 hips within 2 years after implantation. The loosening of uncemented acetabular component was higher as reported by Blumenfeld and Barger (2006), where their results showed 33%

early loosening (<1 year) rate of Sulzer Interop TM acetabular component (Sulzermedia, acquired by Zimmer, Warsaw, In). A 15-years follow-up study by Bliss *et al.* (2011), indicated that survivorship of the femoral component was good. However, the survivorship of the Omnifit-PSL porous coated duel radius acetabular shell (Stryker, Mahwah, NJ) was only 69%. In contrast, a recent study by Garavaglia *et al.* (2011) reported survivorship of 98.8% for the Moescher press-fit acetabular component. Early failure of the metallic acetabular component with a rate of 56.25% (45 out of 80 patients) was also observed by Fabi *et al.* (2012). More recently, large-diameter MoM articulating surface was introduced to prevent dislocation and durability of the acetabular component (Langton *et al.*, 2010; NJR, 2010; Bolland *et al.*, 2011; Bosker *et al.*, 2012; Bernthal *et al.*, 2012). A mid-term clinical results by Bolland et al. (2011) for large-bearing MoM hip replacement indicated 17 revisions required out of 199 hips (185 patients) with a mean follow-up of 62 months. They reported that cumulative survival rate was 92.4%.

An early failure of the ASR XL (DePuy, Warsaw, Ind.) was observed by Bernthal *et al.* (2012) with minimum 24 months follow-up study. Out of 70 hips 12 (17.1%) hip revision performed within 3 years, mainly due to pain (7 revisions), loosening (3 revisions), and squeaking (2 revisions). The study by Steele *et al.* (2011) using same prosthesis implanted in 105 hips after a 2 years follow-up indicated 12% (13 component) acetabular component failure due to aseptic loosening. Published studies indicated that the failure rate of the Duraloc acetabular component is contradictory. Some studies indicated loosening rate of this cup was high 35 to 48% at mean of 2 years clinical study (Stockl *et al.*, 1999; Stoeckle *et al.*, 2005). However, some researcher reported 97 to 100% of these prostheses are still in place after 10 years (Girard *et al.*, 2005; Grobler *et al.*, 2005).

1.4.5 Complications and failure of the uncemented acetabular component

Clinical studies indicate the importance of mechanical factors in acetabular component loosening. Failures of the acetabular components are potentially caused due to wear induced osteolysis (Harries, 1995; MacDonald *et al.*, 1990; Grigoris *et al.*, 1993; Morlock *et al.*, 2008), mal-positioning of the acetabular component (Campbell *et al.*, 2006; De Haan *et al.*, 2008; Hart *et al.*, 2009) and stress shielding induced adaptive bone remodelling (Wilkinson *et al.*, 2001; Wright *et al.*, 2001; Laursen *et al.*, 2007; Meneghini *et al.*, 2010; Mulier *et al.*, 2011). Failure to establish

adequate fixation at the time of surgery may result in the rapid generation of a fibrous tissue layer, allowing wear debris particles to gain immediate access to the bone implant interface. Conversely, establishing and maintaining an effective mechanical fixation at the implant-bone interface may reduce wear debris induced osteolysis (Bhumbra *et al.*, 2000). A mechanically secure implant-bone interface is crucial for the long-term survival of the reconstructed acetabulum. Another cause of long-term failure is due to stress shielding induced adaptive bone remodelling.

The effect of osteolysis was observed more in patients implanted with conventional PE acetabular component as compared to other component, such as cross-linked PE, metallic and ceramic acetabular component (Schmalzried *et al.*, 1994; Hozack *et al.*, 1996; Mallory *et al.*, 2000; Dumbleton *et al.,* 2002; Dumbleton and Manley, 2005; Nieuwenhuis *et al.*, 2005; Park *et al.*, 2005; Howard *et al.*, 2011; Kremers *et al.*, 2012). Earlier follow-up study using 445 hips (421 patients) by MacDonald *et al.* (1990) indicated high rate of acetabular loosening due to wear for patients implanted with cementless non-coated HDPE acetabular component. Owing to the excessive generation of wear particle debris, clinical studies by MacDonald *et al.* (1990) and Grigoris *et al.* (1993) did not recommend the use of uncemented PE acetabular components. The pattern of osteolysis around two different cementless metal-backed cups was observed by Clause *et al.* (2001), in a 10-year follow-up study. These acetabular components, one Arthropor cups (having multiple shell holes) and the other Anatomic Medullary Locking (AML) cups (with no holes), were implanted in 112 and 126 hips, respectively. In their study, osteolysis was observed in 47.3% patients implanted with Arthropor cup and in 47.6% patients implanted with AML cup. Another seven-year follow-up study by Orishimo *et al.* (2003) observed osteolysis in 23 hips out of 56 hips implanted with a Duraloc-100 cup articulating against 28mm femoral head.

In order to evaluate the wear patterns of cementless acetabular components, a clinical follow-up study was performed by von Schewelov *et al.* (2004) for the HA-coated duel radius Omnifit cup, wherein osteolysis was observed in 51 cases out of 154 hips at a mean of six years post-operatively. With the same device implanted in 356 patients (429 hips), Nieuwenhuis *et al.* (2005) reported a high incidence of acetabular osteolysis (in 43% cases) and leading to high revision rate, after a mean follow-up of 60 months. Duffy *et al.* (2004) reported osteolysis was observed in 5 hips out of 84 hips (age: 50 years or younger) for patients implanted with Harris-

Galante uncemented acetabular cup at examining between 10 to 12 years. Two acetabular components were also changed; one due to aseptic loosening and other due to dislocation. Recent clinical studies indicated that the cross-linked PE acetabular component performed better than conventional PE acetabular component, in terms of osteolysis (Howard *et al.*, 2011; Kremers *et al.*, 2012). Ten cases of major osteolysis were observed at follow-up examination ranging from two to five years in patients (age ranging from 20 to 59 years) implanted with cementless hemispherical cobalt chrome acetabular component in total hip arthroplasty (Buechel *et al.*, 1994). More recently, Corten *et al.* (2011) reported only 2% osteolysis for solid trispiked cementless acetabular component in 506 hips at a mean of seven-year follow-up study. A comparative five-year follow-up study was carried out by Underwood *et al.* (2011) to identify the failure rate of ASR and BHR hip components. They reported that the failure rate of ASR acetabular component was considerably higher (12.0%) than BHR component (4.3%), potentially due to edge loading.

Incorrect positioning of the acetabular component in hip arthroplasty results in a higher rate of dislocation as well as increased wear and osteolysis. A series of clinical studies indicated that mal-positioning of acetabular component and cup instability have been associated with excessive wear generations and dislocation of the acetabular component (Sieber *et al.*, 1999; Patil *et al.*, 2003; Campbell *et al.*, 2006; De Haan et al., 2008; De Smet *et al.*, 2008; Langton *et al.*, 2008, 2010; Angadji *et al.*, 2009; Hart *et al.*, 2009; Wysocki *et al.*, 2009). The study by Patil *et al.* (2003) indicated incorrect positioning of the PE acetabular component resulted in high wear rate of the PE component leading to osteolysis. De Haan *et al.* (2008) reported that out of 42 patients who underwent for revision of metal-on-metal resurfacing component, 27 revisions were required due to mal-positioning of the acetabular component, mostly because of excessive abduction angle or anteversion angle. The study by De Smet *et al.* (2008) also reported that the incorrect positioning led to high wear rate of the metallic acetabular component, causing an increase in the serum metal ions levels. Another clinical study by Wysocki *et al.* (2009) reported that 4% acetabular component revisions were required because of mal-positioning.

Stress shielding induced adaptive bone remodelling has been one of the main causes of failure for hard-on-hard bearing surfaces. A series of clinical studies with cementless metallic acetabular implants indicated peri-prosthetic bone resorption

around the pole of the implant (Wilkinson *et al.*, 2001; Wright *et al.*, 2001; Laursen *et al.*, 2007; Meneghini *et al.*, 2010; Mulier *et al.*, 2011), and bone apposition around the acetabular rim (Wilkinson *et al.*, 2001; Wright *et al.*, 2001; Meneghini *et al.*, 2010). The clinical study by Wright *et al.* (2001), reported that the load is transmitted predominantly through the cup to the peripheral cortex of the acetabulum and the ilium, and consequently, the cancellous bone of the central part of the ilium is mechanically shielded. Similar results were predicted by Wilkinson *et al.* (2001). A clinical bone remodelling study around cementless acetabular components by Meneghini *et al.* (2010) observed that relative bone density was increased in the periphery of the acetabulum, due to increased load transfer through that region, whereas bone density decrease was observed around the pole of the implant due to stress shielding. Two types of cementless implant with different material properties were considered to investigate the bone remodelling around the implanted acetabulam, one a solid titanium and other more elastic porous tantalum. Seventeen hips underwent quantitative CT at a mean of 7.7 years, and adjacent bone mineral density (BMD) was calculated using DEXA method. They observed that the relative bone density increased in all regions adjacent to the porous tantalum component from 5 - 40% relative to other implant. However, Laursen *et al.* (2007) observed predominant bone loss (reduction in BMD) within the acetabulum for metallic cups that stabilised over the first post-operative year. More recently, Mulier et al. (2011) also reported bone resorption all over the acetabular region for metallic components.

Apart from bone resorption around the pole of the acetabular component for metallic acetabular components, another concern was raised regarding the long-term clinical effect of metal-ion release from MoM bearings, which may react with body fluid (Clarke *et al.*, 2003; De Smet *et al.*, 2008; De Haan *et al.*, 2008; Langton *et al.*, 2008; Grammatopolous *et al.*, 2009; Hart *et al.*, 2009; Vendittoli *et al.*, 2010; Browne *et al.*, 2010; Levine *et al.*, 2013). In order to overcome this problem, ceramic, cross-linked PE, composite acetabular component appeared to be viable alternative to metallic acetabular component. However, a little is known about the effect of these materials on wear induced osteolysis, bone remodelling around the implanted acetabulum. Mechanical loosening or osteolysis was not observed for cross-linked PE cups, articulating against alumina ceramic femoral head (Wroblewski *et al.*, 2005). None of the alumina ceramic acetabular components failed during a 48-month follow-

up by Bierbaum *et al.* (2002). A similar result was observed by D'Antonio *et al.* (2002) for a mean follow-up period of 35.2 months.

Although ceramic-on-ceramic bearing couples reduce wear, recent evident shows some problem related to ceramic linear fracture and squeaking of the hip (Mahoney *et al.*, 1990; Morlock *et al.*, 2001; Buchanan, 2003; Eickmann *et al.*, 2003; Min *et al.*, 2007; Tateiwa *et al.*, 2008; Restrepo *et al.*, 2008; Jarrett *et al.*, 2009; Taheriazam *et al.*, 2011). The clinical study by Tateiwa *et al.* (2008) indicated first- and second-generation ceramic had a linear fracture rate of 5% to 13%, respectively. A clinical study by Jarrett *et al.* (2009) reported that 14 patients (10.7%) out of 131 patients, who underwent ceramic-on-ceramic hip replacements during the years 2003 to 2005, had an audible squeak during normal walking. Restrepo *et al.* (2008) remarked that the squeaking effect was mainly caused due to component malpositioning. Their study reported that 28 patients (2.7%) have squeaking effect out of 999 patients, who underwent ceramic-on-ceramic hip replacements. More recently, D'Antonio *et al.* (2012) reported that squeaking was observed in 2 cases out of 144 hips with ceramic bearings.

Recent developments in acetabular component design suggest flexible, wear resistant, anatomic shaped components fabricated from polymer composites. A two-year follow-up study on bone remodelling by Field *et al.* (2006) using Cambridge acetabular component (made of CFR-PBT interlock with UHMWPE articulating surface), reported BMD decrease in regions superior and medial to the acetabulum during the first six months, post-operatively. At the inferior side of the acetabulum, BMD decrease was observed until one year after surgery, with no significant changes in bone density thereafter. Despite these clinical studies, the long-term performance of the composite acetabular cups, are yet to be investigated.

1.4.6 Biomechanical studies on intact and implanted pelvic bone

In this section, a review of past studies on intact and implanted pelvic bone, both experimental and numerical (FE) have been conducted.

1.4.6.1 Intact pelvis: FE and experimental studies

Despite few experimental and FE studies (Goel *et al.*, 1978; Carter *et al.*, 1982; Vasu *et al.*, 1982; Pederson *et al.*, 1982; Oonishi *et al.*, 1983; Huiskes, 1987; Dalstra and Huiskes, 1995; Dalstra *et al.*, 1995; Garcia *et al.*, 2000; Thompson *et al.*, 2002;

Majumder *et al.*, 2004; Anderson *et al.*, 2005; Phillips *et al.*, 2007; Cilingira *et al.*, 2007; Zhang *et al.*, 2010; Clarke *et al.*, 2013), load transfer across the pelvic bone remains scarcely investigated, quantitatively. A few earlier studies, based on two-dimensional (2-D) FE models (Carter *et al.*, 1982; Vasu *et al.*, 1982; Rapperport *et al.*, 1985) and assuming axisymmetric structure (Pederson *et al.*, 1982; Huiskes, 1987), are considered to be inadequate, since these simplified models do not account for the out-of-plane geometry and loading conditions.

Three-dimensional (3-D) FE models of the intact pelvic bone were developed and analysed to study load transfer across the pelvis during physiological activities (Oonishi *et al.*, 1983; Dalstra and Huiskes, 1995; Garcia *et al.*, 2000; Majumder *et al.*, 2004; Phillips *et al.*, 2007; Zhang *et al.*, 2010). The 3-D FE model of Dalstra and Huiskes (1995) was developed using CT scan data and considered the effect of twenty two muscle forces and hip-joint reaction force. The model consisted of only 2602 elements and 1862 nodes, which seemed to be a coarse mesh. Their results suggested muscle forces have considerable effect on load transfer across the pelvis. A similar study by Majumder *et al.* (2004), assumed homogeneous material property for the cancellous bone, constant cortical thickness and the hip-joint force distributed directly on the acetabular cavity. Another 3-D FE model of the pelvic bone was developed by Garcia *et al.* (2000) to investigate the effect of boundary conditions on displacement of pelvic bone. However, the model did not consider heterogeneous bone material properties. The effects of mesh size and muscle forces on displacement of the pelvic bone were also not investigated.

The FE analysis of pelvic bone by Phillips *et al.* (2007), using all musculoskeletal loading conditions and ligamental boundary conditions, indicated that the inclusions of muscle forces and ligamental boundary conditions affect load transfer across the pelvis. However, homogeneous bone material property was used for the analysis. Hip-joint reaction force was applied through a spherical femoral head and frictionless contact was assumed between acetabular cavity and spherical head. A recent multi-factorial sensitivity study by Clarke *et al.* (2013) suggested that inclusion of ligamentous boundary conditions at the sacro-iliac and the pubis symphysis joints was not essential, and these could be replaced by rigid constraints for a pelvis FE model. Although a cartilage layer was assumed in their model, the load was transferred through a perfectly spherical head (Clarke *et al.*, 2013). It may be summarised that these models either lack the ability to accurately describe the complex pelvic

geometry or the heterogeneous bone material property distribution. The method of application of hip-joint force in all the models was less appropriate than the physiological condition, since a cartilage layer was not considered in between the anatomic femoral head and the acetabular cavity.

Experimental validation is required to evaluate the correctness of an FE model. Assessment of the validity of the results predicted by 3-D FE models of the pelvis were undertaken by several authors (Dalstra *et al.*, 1995; Anderson *et al.*, 2005; Shim *et al.*, 2008; Leung *et al.*, 2009; Zhang *et al.*, 2010). The bone geometry (contour data and cortical thickness) and material properties of the pelvis FE model of Dalstra *et al.*, (1995) were based on CT-scan data. Load transfer across the pelvic bone was also investigated by Anderson *et al.* (2005) using strain gauge technique and FE analysis. They concluded that the thickness of cortical bone has considerable influence on strain distribution across the pelvis. More recently, Zhang *et al.* (2010) developed and validated a 3-D pelvic bone FE model using homogeneous and heterogeneous cancellous bone material properties. In comparison to the homogeneous model, the results predicted by heterogeneous bone model were found to be in better agreement with the measured strains. However, for all these experiments, a part of the ilium was fixed in a bed of cement resulting in large areas of rigid fixation, which is not representative of the *in vivo* support condition. A recent study on validation of subject-specific pelvis FE model by Hao *et al.* (2011) indicated that the boundary conditions have large influence on load transfer across the pelvis.

1.4.6.2 Implanted acetabulum: FE and experimental studies

Some early FE investigations on implanted pelvic bone were mainly based on 2-D FE models (Carter *et al.*, 1982; Vasu *et al.*, 1982; Rapperport *et al.*, 1985) and axisymmetric structure (Pederson *et al.*, 1982; Huiskes, 1987). Later, more realistic 3-D FE models of the implanted pelvises were developed potentially for investigating the changes in load transfer due to implantation (Dalstra, 1993; Ramamurti *et al.*, 1996; Ries *et al.*, 1989, 1997; Spears *et al.*, 1999, 2000, 2001; Widmer *et al.*, 2002; Thompson *et al.*, 2002; Yew *et al.*, 2006; Jin *et al.*, 2006; Udofia *et al.*, 2007; Manley *et al*., 2006; Janssen *et al.*, 2010; Zhang *et al.*, 2010; Clarke *et al.*, 2012a).

Earlier experimental studies on pelvic bone were mainly focused on strain measurements, without validating the experimental data with some other experiments or FE results (Jacob *et al.*, 1976; Petty *et al.*, 1980; Lionberger *et al.*, 1985; Finlay *et*

al., 1986; Ries *et al.*, 1989, 1999). The study by Lionberger *et al.* (1985) investigated the effect of prosthetic acetabular replacements on strain distributions using strain gauge technique and four types of metallic cemented implants. The effect of strain shielding was observed at different locations on the implanted pelvis. The effect of acetabular material on pelvis cortex strain was experimentally measured by Dickinson *et al.* (2012) using full field strain measurement technique. A digital image correlation (DIC) technique was implemented to measure full-field strain distribution on lateral side of the pelvis cortex. Their results indicated pelvis cortex strain was close to natural pelvis for implantation with CFR-PEEK than metallic (CoCrMo alloy) and UHMWPE. However, they did not compare their results with other measured or numerical data. The experimental study by Small *et al.* (2013) investigated the effect of acetabular cup orientations and implant stiffness on pelvic cortex strain using strain gauge and DIC techniques. Four different implant designs were implanted in composite hemi pelvis with 35 degree and 50 degree abduction angle. Their results indicated change in abduction angle resulted in a 12% increase in cortex strain at medial acetabular wall and an 18% decrease in strain at inferior lateral regions. They also observed that an increase in the stiffness of the acetabular component led to an increase in pelvis cortex strains.

The study by Kluess *et al.* (2009) attempted to validate their FE predicted strain and micromotion using experimental measurement on a fresh human pelvis. Although strain and micromotions were measured using strain gauge and optical markers, micromotion results were not validated due to measurement inaccuracies. However, Zivkovic *et al.* (2010) validated FE predicted micromotion using six LVDTs measured data, under chair-rising loading condition. More recently, FE model validation was performed by Clarke *et al.* (2012b) by measuring strain and micromotion in composite hemi-pelvis model. Four strain rosettes were used for strain measurement and a new technique using digitizing arm was used to measure the micromotion. Good correlation was found between the measured and FE predicted strains and micromotions.

There is a considerable interest in fixation techniques of cementless acetabular components. The success of an uncemented acetabular component is mainly dependent on the biological attachment with bone, which is, in-turn, dependent on the amount of bone ingrowth into the porous coated surface of the implant. The initial fixation of the implant depends on the amount of interference fit (press-fit) at the

acetabulam rim and the coefficient of friction between implant-bone interfaces (Ramamurti *et al.*, 1996; Spears *et al.*, 1999, 2000, 2001; Janssen *et al.*, 2010). A number of FE studies have been performed using press-fit acetabular component to investigate the contact stress, acetabular cup deformation, acetabular strain/stress and implant-bone micromotion (Ramamurti *et al.*, 1996; Ries *et al.*, 1997; Spears *et al.*, 1999, 2000, 2001; Widmer *et al.*, 2002; Yew *et al.*, 2006; Jin *et al.*, 2006; Udofia *et al.*, 2007; Hsu *et al.*, 2007, 2008; Janssen *et al.*, 2010). The FE study by Ramamurti *et al.* (1996) suggested that the limiting value of implant-bone micromotion that inhibits bone ingrowth might vary with the degree of press-fit for reasonable frictional coefficients. A series of FE studies by Spears *et al.* (1999, 2000, 2001), examined the effect of frictional properties and interference conditions on stability and bone ingrowth in an around the implanted acetabulam. A 2-D linear-elastic FE analysis (Spears *et al.*, 1999) suggested friction coefficients varying between 0.2 – 0.3 and an interference fit of 0.25mm for acetabular cup stability. Later, they used a 3-D FE model to investigate potential bone ingrowth on porous coated implant using implant-bone micromotion data (Spears *et al.*, 2000). Excessive micromotion and lack of bone ingrowth was reported in the anterior region and around the pole. Subsequently, they concluded that the best interfacial conditions related to fixation and micromotions was achieved in the press-fit with low interference fit (Spears *et al.*, 2001).

Thompson *et al.* (2002) extended the model developed and validated by Dalstra *et al.* (1995) to represent the pelvis implanted with the acetabular component of various resurfacing prosthesis and fixation conditions. They compared all-polymer hip resurfacing design to MoM design and MoP design. They showed that the implant material appeared to have little effect upon cancellous bone strain failure with both bonded and debonded bone-implant interfaces. A parametric study was performed by Cilingir (2010), using FE analysis to examine the effect of radial clearance, loading, alumina coating on implants, bone quality, and fixation of cup-bone interface on contact pressure and stress distribution of CoC hip resurfacing prosthesis. They observed that a reduction in radial clearance had the dominating effect on contact pressure out of all the parameters. Results of their study indicated that the effect of stress shielding was major causes of concern of this type of prosthesis.

The study by Udofia *et al.* (2007) predicted that the effect of implant-bone interfacial conditions have large influence on implant-bone micromotion, acetabular

stress and contact pressure. Four different implant-bone interface conditions, having 1 mm and 2 mm press-fit, exact fit and fully bonded interface conditions were used in their 3-D FE model. Their results indicated that the maximum micromotion of 60.1 μm was predicted for the FE model with exact fit condition, whereas press-fit condition reduced the micromotion less than 10 μm. Janssen *et al.* (2010) also investigated the effect of interference fit, friction and implant material on stability or fixation of uncemented acetabular prosthesis using different bone quality. Two acetabular prostheses were considered; one flattened acetabular implant with polar clearance and other hemispherical design. They concluded that flattened cup did not significantly improve fixation over hemispherical design in case of poor bone quality.

The effect of bearing materials on contact pressure, contact shear stress, sliding distance and stress/strain distributions in bone structures were investigated by Cilingir *et al.* (2012). They observed that the predicted contact pressure and contact stress were high for CoC material combination, whereas these were low for MoP combination. The predicted sliding distance was low for CoC, CoM and MoM combination, whereas sliding distance was high for CoP and MoP combination. Considering their results, they have concluded that the stress/strain shielding effect associated with ceramic implants appears to be major causes of concern regarding use of this prosthesis. However, in all their models a constant cortical bone thickness and homogeneous material property distribution in the cancellous bone were assumed.

Apart from some clinical studies, bone remodelling around uncemented acetabular component has rarely been investigated using FE formulation. The FE study by Levenston *et al.* (1993) predicted bone loss upto 50% medial to the prosthesis and increased bone density of approximately 30% around the acetabulam rim. The FE study by Manley *et al.* (2006) on acetabular components predicted inevitable bone adaptation that was influenced by changes in design as well as implant material properties. In their study, however, the changes (positive/negative) in bone strain energy density before and after implantation were assumed to cause changes in bone density (formation/resorption), without actually simulating the bone remodelling algorithm.

Acetabular cup thickness and the diameter of the femoral component are known to be important for stresses and wear in acetabular implant. Charnley's early work showed that for a given external diameter, a thick cup and small femoral head led to a

much more uniform stress distribution and lower stresses in the surrounding acetabular bone than a thin cup with a large femoral head (Charnley, 1979). This finding was confirmed by Dalstra (1993), who showed that increasing the PE cup thickness reduced peak stresses in all surrounding materials (bone, PE, cement). Metal-backed PE acetabular cups were originally introduced to facilitate exchange of the PE liner. Some FE studies that used simplified planar or axisymmetric models also predicted that load would be more uniformly transferred with a metal backing. However, this type of cup has a much lower success rate than the conventional all PE cemented cup (Ritter *et al.*, 1990). The FE method was employed by Udofia *et al.* (2004) to study the contact mechanics in metal-on-metal hip resurfacing prostheses, with particular reference to the effects of bone quality, the fixation condition between the acetabular cup and bone, and the clearance between the femoral head and the acetabular cup. Amongst all the factors, the study showed that a decrease in the clearance between the acetabular cup and femoral head had the largest effect on reducing the predicted contact-pressure distribution. It was found that as the clearance was reduced, the influence of the underlying materials, such as bone and cement, became increasingly important.

There are only a few FE studies on wear prediction of PE acetabular components of THA from contact stress and sliding distance, using Archard's equation (Maxian *et al.*, 1996 a, b, c, 1997; Hung and Wu, 2002; Teoh *et al.*, 2002; Kang *et al.*, 2006; Bevill *et al.*, 2005). Results of the study by Maxian *et al.* (1996a) indicated reduction of linear and volumetric wear rates due to decrease in diameter of the femoral components. Similar results were observed by Bevill *et al.* (2005), where volumetric wear rate of the PE acetabular component was decreased due to increase in thickness of the acetabular components. Wear behaviour of a PE acetabular component was investigated by Hung and Wu (2002) using different articulating material composition. They concluded that the articulating material combinations have a large influence on the wear rate. They observed that the ratio of wear between PE/ceramic couples and PE/metal couples was 0.5. Their results also indicated that volumetric wear was decreased due to increase in thickness of the acetabular component. Cosmi *et al.* (2006) reported a FE comparative wear study of two MoM THR systems using Reye hypothesis and presented an approximate analytical model based on Hertz

contact theory. Their results indicated that increase in thickness of the acetabular component resulted decrease in volumetric wear.

The thickness and selection of implant material have played a crucial role in implant-induced bone adaptation and volumetric wear (Maxian *et al.*, 1996 a; Bevill *et al.*, 2005; Cosmi *et al.*, 2006; Scholes and Unsworth, 2007; Scholes *et al.*, 2008). Hence, optimal selection of material and thickness of the acetabular component is necessary to minimize the effects of bone resorption and volumetric wear. However, as compared to the femoral component, optimally designed acetabular component remain relatively under-investigated (Dalstra, 1993; Ong *et al.*, 2006; Matsoukas and Kim, 2009). The single objective design optimization studies by Dalstra (1993) and Matsoukas and Kim (2009) were based on minimization of bone density loss and volumetric wear in PE components, respectively.

1.5 Motivation of the study: unsolved problems

Aseptic loosening of an implanted joint is a process controlled by a number of mechanical and biological factors. It is characterised by the formation and progressive thickening of a continuous fibrous tissue layer between the prosthesis and bone, bone resorption and ultimately migration of the prosthesis. While wear particles debris generated from articulating surfaces and other sources is known to be a contributing factor in acetabular component loosening, clinical evidence supports the role of mechanical factors in the initiation and propagation of failure. Establishing and maintaining a mechanically adequate interface between prosthesis and bone are critical to the long-term stability of the reconstructed acetabulum. Similar to other load bearing prostheses, the mechanical behaviour of the implanted acetabulum, both in the post-operative period and in the long term, depends on the conditions established during surgery and the design of the implant. Long-term failure of acetabular prostheses appears to be dominated by the local tissue response to the altered mechanical environment induced by the prosthesis. Moreover, the biological reaction to wear debris and the long-term response of the prosthesis itself (fatigue failure of the cement mantle if a cemented prosthesis or failure of the porous coating if an uncemented prosthesis) might be other causes of failure.

Failure mechanisms of the acetabular component have been mainly attributed to stress shielding induced adverse bone remodelling and excessive generation of wear particle debris. The extent to which the mechanical factors play a role in the failure

process of cementless acetabular components, however, are not clearly understood yet. The causes of mechanical failure may depend on several factors, such as bone quality, implant design, implant positioning, fixation method and implant-bone interface condition. In order to investigate the stress, strain related failure mechanisms, stress analysis of intact and implanted pelvic bones are required. Before analysing an implanted acetabulum, it is necessary to analyse a healthy functioning hip joint in combination with physiological loading conditions to quantitatively determine the stresses and strain in an intact pelvis, most importantly the acetabulum, and to further evaluate the deviations in load transfer due to implantation.

There is a dearth of experimental data on strain measurement in intact and implanted pelvises, which could be used to identify potential links between changes in strain distribution due to implantation and clinical failure mechanisms of the acetabular component (Dickinson *et al.,* 2012; Clarke *et al.*, 2012b). Experimental measurements using the strain gauge technique have often been employed to validate FE models of intact and implanted bone structures (Dalstra *et al.*, 1995; Anderson *et al.*, 2005; Zhang *et al.*, 2010; Clarke *et al.*, 2012b). Strain gauge measurements yield discrete data, which is an average of the real strains occurring underneath the gauge. Many of these localized measurements are required in biomechanical models, where irregular geometry and material heterogeneity often result in large variation of strain across the structure. Furthermore, if there is a sharp gradient in a strain field, it is unlikely to be captured in discrete experimental measurements. Therefore, experimental data on the full-field strain distributions across the pelvis before and after implantation is necessary. Additionally, a thorough experimental validation of the FE model is necessary to trust the numerical results.

There are only a few biomechanical investigations on the pelvic bone, owing to the complexity of the structure (Dalstra and Huiskes, 1995; Dalstra *et al.*, 1995; Garcia *et al.*, 2000; Thompson *et al.*, 2002; Majumder *et al.*, 2004; Anderson *et al.*, 2005; Phillips *et al.*, 2007; Cilingira *et al.*, 2007; Zhang *et al.*, 2010; Clarke *et al.*, 2013). However, these models either lack the ability to accurately describe the complex pelvic geometry or the heterogeneous bone material property distribution. Also, the method of application of hip-joint force for these FE models was less appropriate than the physiological condition, since a cartilage layer was not considered in between the femoral head and the acetabular cavity. It appears

therefore, the development of a 3-D FE model of the intact hemi-pelvis is necessary to understand load transfer during physiological loading conditions and to investigate the changes in acetabular stresses and strain due to implantation. The intact model can further be used to predict bone remodelling around acetabular components.

It has been well understood that hard-on-hard bearing surface reduces wear. However, peri-prosthetic bone density reduction for this type of bearing surface has been threatening for long term fixation. Moreover, the effect of biomechanical factors on stress shielding and the extent of peri-prosthetic bone adaptation have not been well understood yet. It is well known that interfacial contact condition affect load transfer with an implanted bone structure. However, a little is known about the effects of changes in interface condition on the load transfer and bone remodelling within the implanted acetabulum and its relationship with failure mechanisms. It appears from the literature that the effect of bone remodelling and its relationship with potential failure mechanisms for hard-on-hard hip replacements, using CoCrMo metallic and alumina ceramic acetabular components, are not entirely understood. Hence, it is necessary to investigate adaptive bone remodelling and the extent to which the evolutionary changes in stress / strain distribution affect the potential risk of implant fixation failure.

Recent developments in acetabular component suggest acetabular components fabricated from polymer composites, such as CFR-PBT and CFR-PEEK. These flexible composite cups would cause more deformation and less peri-prosthetic bone loss than metal-backed PE, metallic and ceramic hemispherical components (Field and Rushton, 2005; Field *et al.*, 2006, 2008; Manley *et al.*, 2006; Latif *et al.*, 2008; Dickinson *et al.*, 2012), since its elastic modulus (E) is close to bone and it offers the potential to fabricate components with specific requirements (Field *et al.*, 2008). However, the effects of these composite materials and geometry of the acetabular components on bone remodelling within the acetabulum are not clearly understood yet. It is therefore, hypothesized that the choice of implant material, geometry and implant-bone interface conditions affect strain shielding and bone remodelling.

It has been observed that the selection of implant materials and thicknesses has large influence on acetabular component failure due to bone resorption and volumetric wear. Employing a hard-on-hard bearing surface causes reduction in wear, but increase in peri-prosthetic bone resorption (Wilkinson *et al.*, 2001; Wright *et al.*,

2001; Laursen *et al.*, 2007; Meneghini *et al.*, 2010). In contrast, using a PE acetabular cup led to minimal changes in bone density, but excessive generation of wear debris (Harris, 1995). Apart from the implant material, thickness of the acetabular component influences the bone remodelling process and the volumetric wear; an increase in thickness exacerbated bone resorption, but led to decreased volumetric wear (Maxian *et al.*, 1996a; Hung and Wu, 2002; Bevill *et al.*, 2005; Cosmi *et al.*, 2006). The optimal selection of acetabular component material and thickness is, therefore, necessary to minimize the effects of bone resorption and volumetric wear.

Despite the generally inferior clinical performance of acetabular components as compared to femoral components, stress analysis of the acetabular reconstruction, particularly with reference to the effects of prosthesis design variables, remains scarcely investigated. Finite Element (FE) Analysis has evolved as an effective preclinical testing method in orthopaedic research to test and validate clinical hypotheses. Using realistic FE models of bone and implanted bone structure, detailed understanding of the load transfer in an intact pelvis and the same implanted with acetabular prosthesis is certainly required. It is also necessary to investigate the effect of a limited number of design variables on the eventual failure mechanisms of acetabular components. Overall, it seems necessary to thoroughly investigate the load transfer in an implanted acetabulum, in order to gain an insight into the failure mechanisms and to suggest measures for improved acetabular component design.

1.6 Objectives and scope of the study

The primary goal of the study is to develop an improved acetabular prosthesis. Therefore, the study is aimed at investigating the load transfer in an intact and implanted hemi-pelvis with regard to potential failure mechanisms of acetabular component. Analysis of the failure mechanics may suggest measures for optimized acetabular prosthesis design. This study deals with stress distributions in the intact and implanted pelvises, using numerical and experimental methods, and critically examines the extent to which evolutionary changes in bone density and strain pattern relate to the eventual risk of failure. However, the effect of damage accumulation in the implant bone structure has not been considered. The present study consists of the following specific objectives, which collectively contribute towards achieving the primary goal of the thesis:

- Development and experimental validation of FE models of intact and implanted hemi-pelvises and prediction of potential effects of implantation through a comparison of intact and implanted bone strains and measurement of implant-bone micromotion.
- Assessment of the validity of the FE predicted full-field strain distribution in the intact and implanted composite hemi-pelvises and investigations on the effect of deviations in load transfer due to implantation.
- Finite element analysis of a hemi-pelvis during normal walking; investigations on the effect of inclusion of cartilage layer on acetabular stresses and strain.
- Investigations on the deviations in load transfer due to implantation and bone adaptation around cementless metallic and ceramic acetabular components.
- Investigations on the extent of bone remodelling around composite acetabular components having different geometries, material properties and implant-bone interface conditions.
- Determination of the optimal design parameters for the acetabular prosthesis that would minimize bone density loss and volumetric wear using genetic algorithms.

1.7 Structure of the thesis

The present study is focused on biomechanical analysis of stresses and strain in intact and implanted pelvises. The mechanical consequences of inclusion of cementless acetabular components on the acetabulum, and as a whole on the pelvic bone, have been investigated with regard to failure mechanisms. The FE method has been used as the basic tool for pre-clinical analysis. Rigorous experimentations were carried out on composite hemi-pelvises (intact and implanted) models to measure strains using strain gauge and DIC technique, and implant-bone micromotion using linear displacement sensor. These measurements were used to assess the validity of the generated FE models of the intact and implanted hemi-pelvises. The effect of implant induced bone remodelling has been investigated to evaluate the long-term survival of the different acetabular components having variable implant-bone interfacial conditions. This chapter, Chapter 1, deals with general introduction, including literature review, motivation, and objectives of the study. The scopes of other chapters of the thesis, which collectively contribute towards achieving the primary goal of this study, are presented in the following order.

Chapter 2 deals with the experimental validation of numerically (FE) predicted strain and micromotion of intact and implanted composite hemi-pelvises. A new experimental set-up was developed, in order to measure surface strain using strain rosette fixed at different locations and orientations, and to measure implant-bone micromotions along three mutually perpendicular directions using linear displacement sensor. These experimental results were compared to equivalent FE predicted results for different loads, for a rigorous validation of the FE results.

Experimentally measured full-field strain using DIC technique was used for a thorough validation of FE models of intact and implanted pelvises in Chapter 3. The measured full-field strain was compared with FE predicted results at comparable location for the intact and the implanted composite hemi-pelvises. Subsequently, deviations in load transfer due to implantation are also investigated.

In Chapter 4, an elaborate description on the development of a patient-specific FE model of the intact hemi-pelvis using CT-scan data and musculoskeletal loading conditions is presented. An appropriate method of application of the hip-joint force was determined by inclusion of the cartilage layer between the femoral head and the acetabular cavity. Estimates of acetabular stresses and strain have been obtained during normal walking, which serve as a reference solution for comparing deviations in stresses and strain due to implantation. The study is useful to understand load transfer across the hemi-pelvis, in particular the acetabulum, and for further investigations on acetabular prosthesis.

The implant induced bone remodelling around uncemented metallic (CoCrMo alloy) and alumina ceramic acetabular component is presented in Chapter 5. The effect of deviations in load transfer due to implantation, implant-bone micromotion and implant-bone interface failure have also been investigated. A submodel of the implanted pelvis FE model and time-dependent bone remodelling algorithm was developed to investigate changes in bone density distribution around the implanted acetabulum. Adaptive bone remodelling for both these acetabular components have been compared and evaluated in this chapter.

In Chapter 6, the effect of using composite acetabular cup on load transfer and bone remodelling around acetabular components have been investigated. Using FE analysis in combination with the bone remodelling algorithm, this chapter investigated deviations in load transfer and the extent of bone remodelling around

composite acetabular components, having different geometries, material properties and implant-bone interface conditions. The FE study was used to evaluate the most appropriate design of composite acetabular cups with regard to strain shielding, bone deformation and bone remodelling.

In Chapter 7, an optimization procedure was carried out to find out a combination of suitable thickness and material of the acetabular component that would minimize both the bone density loss and volumetric wear. A new method was implemented to determine the objective functions, based on which a mixed-integer multi-objective optimization was formulated. Genetic algorithm (GA) was used for solving this multi-objective optimization problem.

Finally, in Chapter 8: conclusions, the significance and major contributions of the study are presented. These overall conclusions have been drawn based on the results of each chapter. A retrospective review on the outcomes of the thesis and recommendations for future research on acetabular components have also been presented.